

## REVIEW

[View Article Online](#)  
[View Journal](#) | [View Issue](#)



Cite this: *J. Mater. Chem. B*, 2025, 13, 8953

## From simple delivery to multimodal systems: the critical role of macromolecular platforms in bioorthogonal drug synthesis

Tieze van den Elsen  and Kevin Neumann  \*

Targeted drug delivery strategies have emerged as promising solutions to overcome traditional challenges such as poor bioavailability and side effects associated with conventional drug delivery methods. Among these strategies, the use of prodrugs offers a viable approach by leveraging enzymatic or controlled chemical transformations *in vivo* to enhance drug efficacy and specificity. The advent of bioorthogonal chemistry has revolutionized prodrug activation, providing a multitude of activation strategies beyond conventional methods. This review explores the integration of bioorthogonal chemistry, particularly transition metal catalysis, into prodrug activation strategies, with a focus on the use of macromolecular scaffolds as platforms to enable and localize these chemistries in biological environments. Specifically, this review focuses on the growing field of *in situ* bond-forming synthesis mediated by transition metal catalysts, often enabled by the use of macromolecular platforms. By forming carbon–carbon or carbon–heteroatom bonds intra- or intermolecularly, this approach offers advantages over traditional uncaging strategies through the absence of the pharmacoactive motif in the prodrug. We emphasize the central role of macromolecular platforms in integrating bioorthogonal chemistries into multimodal systems that enable targeting strategies and stimuli-responsive behavior, both crucial for achieving site-specific activation and minimizing off-target effects. We conclude that the future of this field lies with the development of retrosynthetic prodrug design, and the use and development of multimodal macromolecular platforms to host and enable new bioorthogonal transition metal catalysis.

Received 9th May 2025,  
Accepted 27th June 2025

DOI: 10.1039/d5tb01111f

rsc.li/materials-b

*Institute for Molecules and Materials, Radboud University, The Netherlands. E-mail: kevin.neumann@ru.nl*



**Tieze van den Elsen**

*further academic career as a PhD candidate in the group of Nobel Laureate Professor B. L. Feringa exploring smart surfaces and adaptive materials.*

*Tieze van den Elsen holds an MSc in Chemistry with expertise in organic, inorganic, and supramolecular chemistry. He earned both his Bachelor's and Master's degrees cum laude from Radboud University Nijmegen. During his Master's studies, he completed research internships with Professor R. J. M. Nolte at Radboud University, the Netherlands, and Professor R. A. Shenvi at The Scripps Research Institute in San Diego. From 2025, he pursues his*



**Kevin Neumann**

*Zurich, Switzerland, where he focused on developing new methodologies for peptide synthesis. Since 2021, Kevin has been an Assistant Professor in Nijmegen, the Netherlands, where he leads an interdisciplinary research group at the interface of organic and polymer chemistry. His work focuses on the development of next-generation drug delivery systems and the precision synthesis of therapeutically active biomolecules including protein–polymer conjugates.*



## 1. Introduction

Traditional drug delivery methods are riddled with various challenges. Besides drug efficacy, the most important challenges to overcome are those relating to bioavailability and reduction of side effects. The latter is especially important in cases such as traditional chemotherapy where severe side effects are often observed due to lack of tissue specificity.<sup>1</sup> To address these challenges, targeted drug delivery strategies have emerged as promising solutions. These strategies aim to deliver drugs directly to the site of action, thereby minimizing off-target effects.<sup>2</sup> The concept of 'prodrugs' is one of the strategies developed to minimize the undesirable properties of drugs. Prodrugs are inactive, derivatives of active drug molecules, that can be transformed *in vivo* via enzymatic or chemical ways to form the active parent drug. The use of prodrugs can improve bioavailability and distribution as well as improve selectivity for the desired target and thereby reduce side effects. Widely known examples of the first use of prodrugs include methenamine, a urinary tract site selective prodrug for antibacterial formaldehyde, and aspirin, the acetylated and less irritating precursor of sodium salicylic acid.<sup>3</sup> The most common method of prodrug activation is that of endogenous stimulation *via* microenvironmental factors such as pH and localized concentrations of biomolecules, or transformation *via* specific proteins. However, complete specificity and selectivity are difficult to obtain because of the limited differences between healthy and malignant tissues. Small amounts of transformation of the prodrug at off-target sites might still lead to significant side effects.<sup>4</sup> Additionally, full spatiotemporal control is difficult to obtain due to the dependence on endogenous activation.

A huge advancement in the field of medicinal chemistry was the introduction of 'bioorthogonal chemistry' by Bertozzi in 2003.<sup>5</sup> This Nobel prize winning chemistry refers to chemical reactions that occur selectively within living systems without interfering with native biological processes. Early and most famous examples of bioorthogonal chemistry include the Staudinger ligation, and 'click chemistry' such as the copper-catalyzed azide-alkyne cycloaddition (CuAAC), the strain-promoted azide-alkyne cycloaddition (SPAAC), and the inverse-electron demand Diels-Alder (iEDDA) reaction. Many more reactions have been reported since.<sup>6</sup> Nowadays, one of the main uses of bioorthogonal reactions, is the activation of prodrugs (Fig. 1). The main advantage of using bioorthogonal chemistry for prodrug activation is that it adds an extra layer of controlled administration over regular endogenous activation, resulting in higher prodrug selectivity and specificity. Many bioorthogonal chemistry mediated prodrug activation strategies are focused on uncaging/deprotection reactions. These reactions have the purpose of cleaving a bond, revealing the active drug molecule *via* unmasking, cleavage of linkers, or release of payload.<sup>7</sup> For this purpose, bioorthogonal reactions often rely on the concept of 'click-to-release'. These are modified ligation reactions with the formation of an unstable intermediate product, leading to dissociation of the drug molecule. Examples of this entail modified Staudinger ligations, iEDDA reactions with tetrazines, and modified SPAAC reactions with *trans*-cyclooctenes.<sup>7</sup>

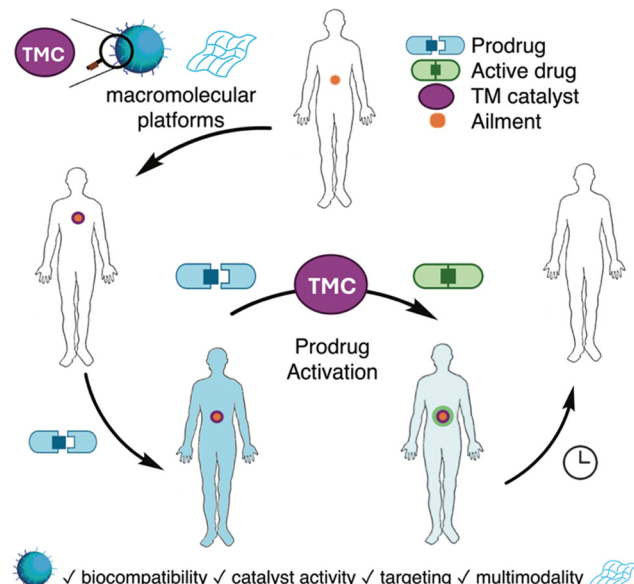


Fig. 1 Schematic representation of transition metal catalyst (TMC) mediated *in situ* prodrug activation strategies. With the help of functionalized macromolecular platforms, the TMC accumulates at the site of the ailment. Then the non-active prodrug is distributed in the body and selectively activated near the ailment. This happens through bond formation catalyzed by the TMC. The activated drug only effectuates in the vicinity of the ailment only and over time cures it.

The use of transition metal catalysts (TMCs) has become indispensable in all fields of synthesis over the last few decades, owing to their metal properties and versatile reactivity patterns in various transformations.<sup>8</sup> The translation of TMCs into biorelevant environments for safe and selective catalysis *in cellulo* and *in vivo* to modulate cellular functions and introduce new-to-nature transformations to living systems, is a field of research with high potential for novel selective and efficient therapies and *in vivo* imaging. However, the translation towards bioorthogonal transition metal catalysis is faced with several challenges. Metal complexes often require water- and oxygen-free environments to prevent deactivation. In biological systems, they are confronted with many chelating and nucleophilic biomolecules such as amines and thiols, which can efficiently alter and deactivate the catalytic nature of the metal complexes and promote their excretion from the body. Additionally, some transition metals used in catalysis express toxicity towards cells.<sup>9</sup> Despite these challenges, various bioorthogonal TMCs have been reported for *in cellulo* and *in vivo* catalyzed transformations, such as ligations, uncaging/deprotection reactions, oxidations, reductions and bond formations.<sup>10</sup>

While early efforts in bioorthogonal chemistry predominantly relied on small molecules or antibody-drug conjugates for prodrug activation, a limited number of pioneering studies have demonstrated the potential of macromolecular scaffolds to facilitate bioorthogonal transformations. Although, strictly not drug activation nor synthesis, in 2012, R. Weissleder and co-workers reported the use of biomacromolecular scaffolds in



form of dextrans decorated with tetrazine residues for cellular resolution imaging and  $^{18}\text{F}$  labelling of biological target.<sup>11</sup> In this study, pre-targeting was achieved by using anti-CD45 monoclonal antibodies labelled with dienophiles. The authors observed significantly enhanced *in vivo* labelling when polymer-tetrazine conjugates were employed instead of small molecule analogues. During the early phase of translating bioorthogonal chemistries to more complex environments, this study was among the first to employ a macromolecular scaffold in conjunction with bioorthogonal reactions and certainly inspired others to develop more functional macromolecular platforms that support bioorthogonal chemistry.

Since then, macromolecular platforms including polymeric nanoparticles, biomacromolecular networks, and protein conjugates, have evolved beyond passive delivery vehicles to incorporate intrinsic reactivity within their frameworks. Among other features, these systems offer compartmentalization and spatial resolution, enabling selective drug synthesis *via* bioorthogonal chemistry. The chemistry and architectures of such macromolecular platforms is vast, and includes besides some frequently used polymers such as polyethylene glycol, polyoxazoline and polysaccharides<sup>12</sup> more tailored structures including poly(ylides),<sup>13,14</sup> polymeric *n*-oxides<sup>15</sup> and poly allyl glycolyl ether<sup>16</sup> of which many are of interest for enabling new TM catalytic systems.

A major challenge in conventional therapy is the issue of site-selectivity which also applies to bioorthogonal drug synthesis. Besides acting as a synthetic platform for catalyst immobilisation, macromolecular scaffolds can be used to overcome site-selectivity issues. For example, one strategy to overcome this challenge involves the integration of exogenous trigger-responsive functionalities into macromolecular platforms. Unlike traditional small molecule-based systems, macromolecular drug delivery

platforms such as polymeric nanomedicines offer inherent multimodality, enabling the incorporation of additional functional elements without the need to synthetically modify the bioactive payload.

When applied to prodrug activation strategies, most reported bioorthogonal TMCs are used in uncaging/deprotection reactions mainly focused on dealkylations such as ruthenium and palladium promoted deallylations, and palladium, gold and platinum mediated depropargylations.<sup>17</sup> Using this strategy, bioactive functional groups (*e.g.* amines, hydroxides, or acids) are unmasked resulting in a bioactive molecule.

A more recently investigated method for prodrug activation is *in situ* bond-forming synthesis, where the focus lies on the formation of C–C or C–X (X = heteroatom) bonds resulting in the active drug rather than breaking bonds for unmasking. These reactions include various cycloadditions, cross-couplings, and metathesis reactions promoted by a variety of transition metals (Cu, Pd, Ru, Au, Rh, Ir). The TMC promoted reactions provide a wide range of possible chemical reactions, leading to a large amount of prodrug activation possibilities.<sup>10</sup> Theoretically, this strategy has an additional advantage over decaging strategies, since the pharmacoactive motif does not yet exist in the prodrug molecule, resulting in a lower bioactivity of the prodrug compared to the bioactive drug, thereby significantly enhancing the therapeutic window. In addition, premature activation is prevented because of the lack of pre-existing drug scaffolds, and thus less side effects.<sup>18</sup>

In this review, the advances in the field of *in situ* TMC mediated bond-forming synthesis are discussed, from its conceptualization and first proofs of concept in 2016, to the most recent discoveries and applications in the present day. Furthermore, the crucial role of macromolecular platforms in enabling these strategies will become clear from the given examples (Table 1). In the first part

Table 1 Overview of selected examples of macromolecular platforms discussed in this review

Ref.	Macromolecular platform	Catalyst	Size of platform [nm]	Multimodality	Synthetic target
19	TentaGel resin	Cu	$16 \times 10^4$	Injected delivery	Combretastatin A4
20	Cross-linked lipoic acid NP	Cu	97	Increased activity by NP shape	Resveratrol analogue
21	Single-chain metal–organic NP	Cu	7	Dual role as ligand and crosslinker	Bisamidine scaffold
22	Polymeric NP	Cu	100	Affinity for localisation at cell membrane	Fluorophore
23	Zr MOF	Cu	120	Mitochondrial targeting	Fluorophore
24	Zn/Cu MOF	Cu	120	DNAzyme co-delivery	Resveratrol analogue
25	ZIF-8 copper chaperone mimics	Cu	62	FA-targeting and dual <i>cis</i> -platin delivery	Resveratrol analogue
26	CuAl-LDH nanosheets	Cu	Lateral size of 140–250 nm	CuAAC and Fenton-like reaction	resveratrol analogue
27	DNA–Cu-NP	Cu		ROS production and co-delivery of DNAzyme	Resveratrol analogue
28	Polystyrene microsphere	Pd	500	Milestone as first reported system	Rhodamine 110
29	Pd(0)-microsphere	Pd		Triggered endocytosis	PP-121
30	Hollow Si-microspheres	Pd	500	Encapsulation of metal catalysts	Fluorophore
31	PLGA–PEG polymeric NP	Pd	57	EPR and stealth effect	Fluorophore
32	Biotin–streptavidin complex	Ru	N/A	Increased activity by tailoring biomolecular environment	Fluorophore
33	Human serum albumin complex	Ru	N/A	Targeting residues	Umbelliprenin
34	Glycosylated albumin complex	Au	N/A	Targeting residues	Phenanthridinium
35	Glycosylated albumin complex	Au	N/A	Targeting residues	Dehydro-pyrrolizidine alkaloids



of this review, we focus on the different chemistries and strategies for *in cellulo* and *in vivo* synthesis categorized by transition metal, and their applications towards *in vivo* therapy. This is followed by a brief overview of examples utilizing exogenous triggers to induce catalytic activity obtaining enhanced spatiotemporal control. Next, an overview is given of different modes of application of the most advanced examples in the field, where *in situ* catalysis is combined with targeting strategies to effectuate target specific catalysis and prevent off-target effects. Finally, the direction of this emerging field and promising new directions according to the authors are highlighted.

## 2. Bioorthogonal *in situ* drug synthesis

### 2.1 Copper catalysis

Copper is a very versatile catalyst in organic synthesis, (co)-catalyzing various reactions such as the Ullmann coupling,<sup>36</sup> Sonogashira coupling,<sup>37</sup> Buchwald–Hartwig amination,<sup>38</sup> and Huisgen 1,3-dipolar cycloaddition reactions.<sup>39</sup> Of these examples the best known Cu catalyzed reaction is the Huisgen 1,3-dipolar cycloaddition inspired Nobel prize-winning copper-catalyzed alkyne–azide 1,3-dipolar cycloaddition (CuAAC) or “click” reaction, pioneered by Sharpless in 2001.<sup>40</sup> This reaction selectively forms 1,4-disubstituted 1,2,3-triazole products with high catalytic efficiency, and moreover in bioorthogonal fashion since the substrates are not naturally found in biological systems. Therefore, this reaction has high potential for *in vivo* applications.

Although copper is considered an essential metal for living organisms as enzymatic cofactor, copper can exert high cytotoxic properties relating to the generation of radical oxygen species (ROS) inducing oxidative stress, and interference in biological pathways.<sup>41,42</sup> To overcome the cytotoxicity and

improve kinetics and efficiency, innovative approaches are required and many studies have been conducted using macromolecular platforms to protect the biological surrounding from undesired toxicity.<sup>43</sup> Hence, macromolecular platforms are not only essential for enhancing catalytic efficiencies but also for providing safe and viable therapeutic platforms.

**2.1.1 Polymeric enzyme mimics.** Early on, copper cytotoxicity shielding was done through embedding copper nanoparticles (Cu-NPs) in polymeric resins (Fig. 2). One of the first examples was presented by Bradley in 2016.<sup>19</sup> The group synthesized entrapped copper nanoparticles (E-Cu-NPs) in a polystyrene poly(ethylene glycol) resin (TentaGel, ~160  $\mu$ m) and showed its biocompatibility through CuAAC promoted formation of coumarin from azide and alkyne precursors resulting in fluorescence in phosphate buffered saline (PBS), 5% fetal bovine serum (FBS) and HeLa cell lysate with full conversion within 3 h. In *in vitro* experiments, the biocompatible catalyst was able to efficiently promote the CuAAC reaction in the extracellular matrix, forming a mitochondrial targeting triphenyl phosphonium (TPP) functionalized coumarin, which was readily taken up by the cells resulting in mitochondria targeted fluorescence. Additionally, the catalyst was able to synthesize a combretastatin A4 (CA4, **1**) derivative, known for its high cancer cytotoxicity, resulting in a 70% decrease in cell viability (HeLa cells) over 3 days, indicating its potential for anti-tumor therapy.

To increase catalyst selectivity, stability, and efficiency, transition metal catalysts have been incorporated in macromolecular scaffolds much like metalloenzymes. An early example of this was presented by Zimmerman in 2016 who employed a single chain linear polymer (SNCP) that was ‘folded’ with covalently bound Cu(II) atoms. The polymer was accessed *via* ring-opening metathesis and formed a water-soluble, copper-cross-linked single-chain metal–organic nanoparticles (MONP’s).<sup>21</sup>

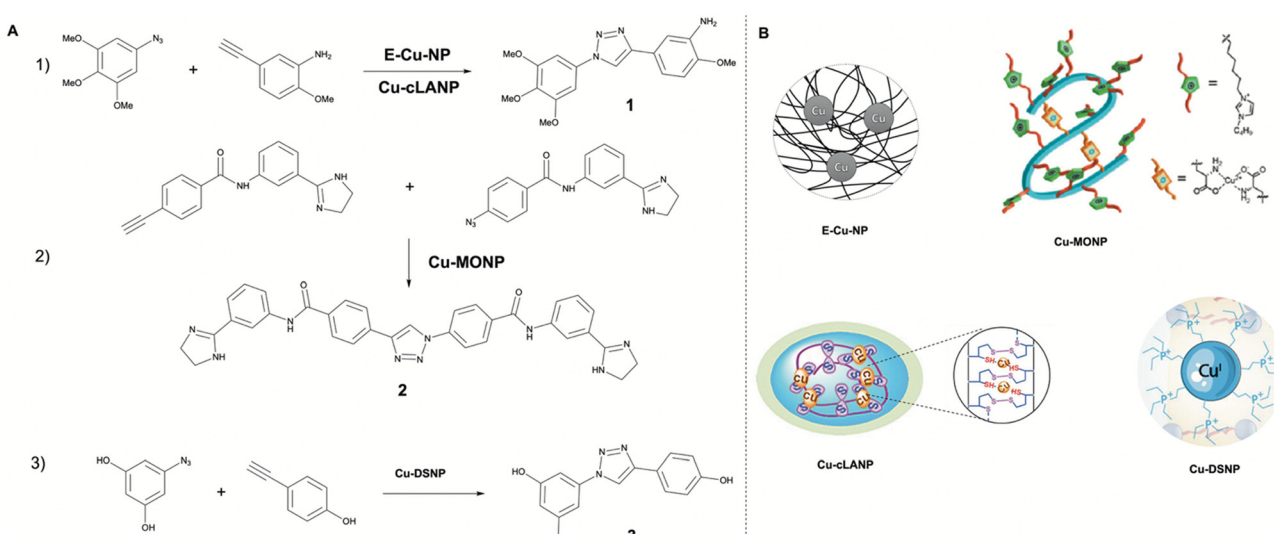


Fig. 2 Overview of reported *in situ* copper catalyzed click-reactions (A) by the respective copper polymeric enzyme mimics (B). (1) E-Cu-NP<sup>19</sup> and Cu-cLANP<sup>20</sup> catalyzed formation of combretastatin A4 (**1**). (2) Cu-MONP<sup>21</sup> catalyzed formation of antimicrobial agent **2**. (3) Cu-DSNP<sup>22</sup> catalyzed formation of resveratrol analogue **3**. Partly reproduced from ref. 20–22 with permission from the American Chemical Society.



The **Cu-MONPs** were tested for their ability to catalyze CuAAC in water using sodium ascorbate to reduce the Cu(II) to Cu(I) *in situ*, resulting in a substrate conversion of >99% within 24 h using only 2.5 ppm of the **Cu-MONPs** in a model reaction. Various other substrates were also tested and resulted in isolated yields ranging from 83% to 98% at 5–30 ppm **Cu-MONPs** after 24 h at 50 °C. It was indicated that the **Cu-MONPs** were significantly less efficient towards hydrophilic substrates indicating the importance of hydrophobic binding. To show biocompatibility, the **Cu-MONPs** were successfully applied in an intracellular fluorescence study using fluorogenic coumarin precursors in live human cancer cells resulting in intense fluorescence. Additionally, the **Cu-MONP** was applied towards the synthesis of an antimicrobial agent 2 in *E. coli* bacteria effecting growth inhibition.

Further structure–activity studies using fluorogenic click reaction and dye uptake experiments conducted on the **Cu-MONPs** revealed the mechanism of its high catalytic efficiency and effectiveness to involve an enzyme-like substrate binding process. It is primarily governed by the hydrophobic character of the substrate and the polymer and works best with a medium sized (19 kDa) MONPs.<sup>44</sup> Although further research was conducted by Zimmerman on **Cu-MONPs** with differentiation towards surface protein binding catalysis<sup>45</sup> and extracellular drug screening,<sup>46</sup> no further application towards *in vivo* drug synthesis has yet been conducted.

Another example of a copper crosslinked polymeric nanoparticle was presented by Zhang in 2018.<sup>20</sup> The Zhang group showed that an important element of nanocatalysts is not only reactivity and biocompatibility but also morphology. Nano-copper-doped cross-linked lipoic acid nanoparticles (**Cu-cLANPs**) of different sizes and shapes were synthesized. In a fluorescence study it was found that the intracellular CuAAC catalytic activity of the larger (~97 nm) rugby-shaped nanoparticles was higher (up to 1.54×) than that of the smaller (47 and 11 nm) spherical nanoparticles. The same trend was found for the cellular uptake rate (up to 1.5×). A cell viability study of *in situ* generated resveratrol analogue 3 *via* CuACC promoted click reaction was conducted with the **Cu-cLANPs**, resulting in cancer cell apoptosis (HeLa cells). Again, the rugby-shaped nanoparticle performing the best at every substrate concentration.

In a continuation on this study, Zhang presented a new application of the cLANPs in 2021.<sup>47</sup> The group constructed Cu-NP and prodrug loaded nanocapsules from cross-linked lipoic acid (cLANCs), which could release their contents upon arrival in the tumor tissue due to glutathione (GSH) over-expression induced degradation. Besides the *in situ* CuAAC promoted CA4 prodrug activation, the cLANCs could be degraded into dihydrolipoic acid (DHLa) which showed a synergistic anticancer effect with the CA4 analogue. It was shown that the system displayed very little activity in a blood environment (1.4% drug yield) but strong activity in tumor environments (84% drug yield), due to the GSH induced release. It also showed good tumor accumulation (up to 11.3× higher than liver), and excellent tumor inhibitory rate (TIR, 83%) in an *in vivo* mice study, being much higher than directly administered CA4 derivative (TIR, 49%). Using the

delivery vesicle in a synergistic antitumor therapy as done in this study shows potential.

Another polymer based macromolecular catalyst was reported by Bai in 2019.<sup>22</sup> The group created a dense-shell nanoparticle (DSNP) scaffold consisting of a positively charged surface and hydrophobic interior with a core containing a high concentration of ligand moieties. This ligand core was able to readily coordinate Cu and Pd atoms and hereby the DSNP could contain and protect the catalytic function of these metal catalysts. The system showed enzyme-like catalysis through a bind-to-catalyze mechanism. It was found *via* fluorescence formation that the DSNP scaffold provided an inherent cell membrane targetability due its amphiphilic structure which caused it to attach to and reside within the lipid bilayer. A follow-up study from 2023 showed that because of this membrane affinity, the DSNP catalyst poses an ideal membrane-embedded catalyst (MEC).<sup>48</sup> The MEC was useful for the synthesis and intracellular delivery of molecules with low cell permeability such as lipophilic or anionic substrates. This was shown *via* an *in vitro* cell viability study comparing the MEC promoted CuAAC click reaction of a proresveratrol analogue, and the extracellular addition of the preformed resveratrol analogue. This resulted in a lower cell viability (35% vs. 61% at 20 μM substrate and analogue, HeLa cells), indicating improved cellular uptake. Additionally, they show the MEC promoted ligation and delivery of a large, anionic cell autophagic agent with a 2-fold efficiency increase compared to the direct extracellular addition of the same agent. This approach is a promising example of the benefits of *in situ* drug synthesis promoting higher intracellular availability. However, because of non-specific membrane targeting a direct *in vivo* approach is still hard to imagine.

**2.1.2 Metal organic frameworks.** Metal organic frameworks (MOFs) are porous materials consisting of linked inorganic and organic units, resulting in highly structured particles with excellent size control and high surface area (Fig. 3).<sup>49</sup> Using MOFs as an approach for CuAAC promoted *in situ* drug formation was presented by Qu in early 2019.<sup>23</sup> The group presented a copper-functionalized MOF that could promote the CuAAC click reaction in live cells. The MOF consisted of a zirconium metal–organic scaffold doped with Cu nanoparticles (10.6 wt%) and functionalized with TPP vectors for mitochondrial targeting (**Cu-MOF-TPP**). The catalytic activity of the Cu-MOF for the CuAAC reaction was shown in water, through the activation of a coumarin derived pro-fluorogenic molecule, resulting in bright fluorescence with a conversion of 80% after 8 h. The reusability and stability of the catalyst was confirmed in various aqueous and biologically relevant media (PBS, cell culture medium). The Cu-MOF could be readily endocytosed in human breast adenocarcinoma (MCF-7) cells and showed negligible cytotoxicity up to 100 μg mL<sup>-1</sup>. A resveratrol analogue (3) was identified as a suitable CuAAC catalytic product with cancer chemopreventive properties. The precursor molecules, with no significant cytotoxicity, were readily converted to the resveratrol analogue inside MCF-7 cells with the use of the Cu-MOF, resulting in significant reduction in cell viability



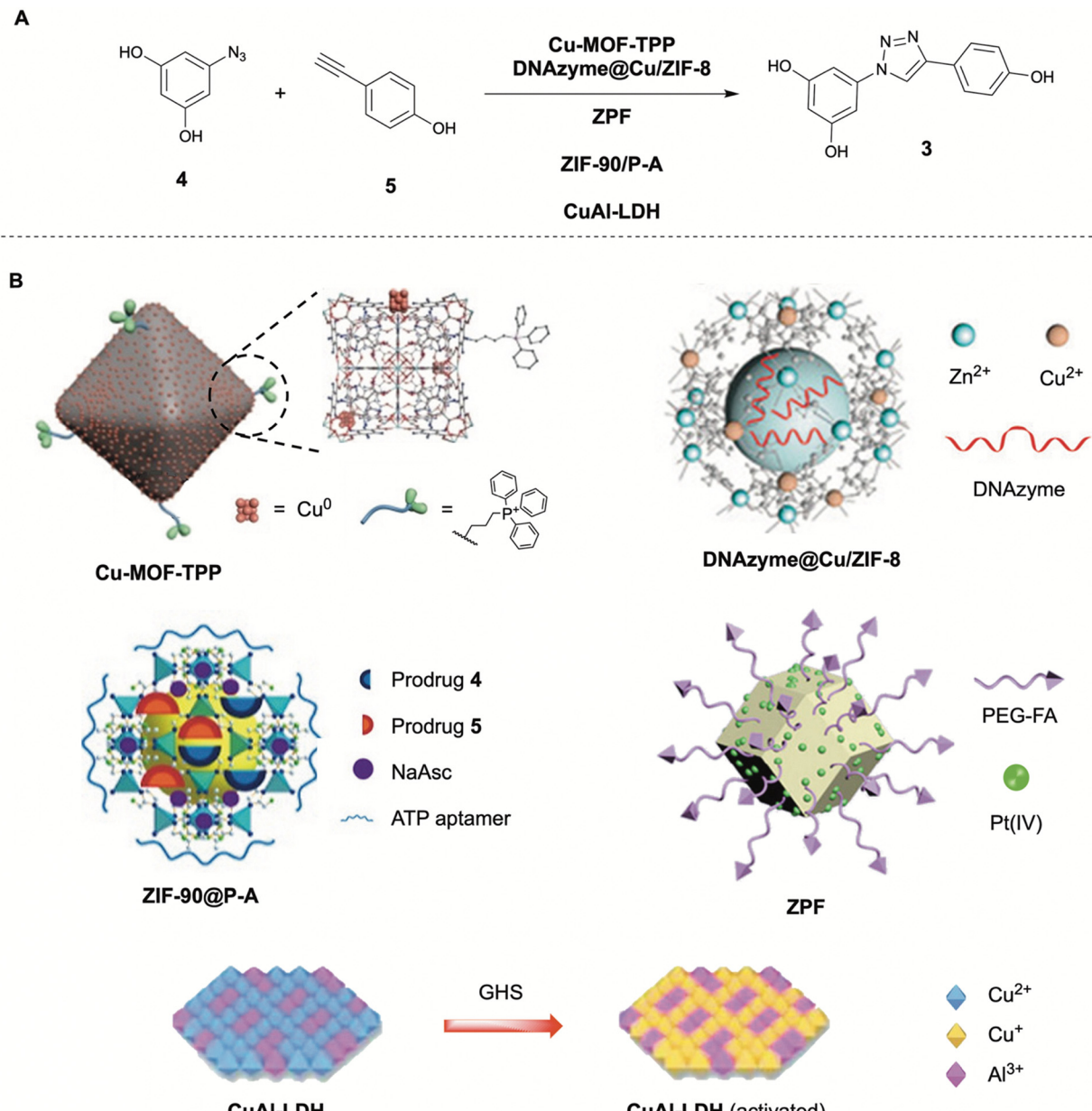


Fig. 3 Reported *in situ* copper catalyzed click-reaction (A) and respective copper functionalized metal organic frameworks (MOFs) (B). (A) Formation of resveratrol analogue **3** from prodrug fragments **4** and **5** via CuAAC by various MOFs (**Cu-MOF-TPP**,<sup>23</sup> **DNAzyme@Cu/ZIF-8**,<sup>24</sup> **ZPF**,<sup>25</sup> **ZIF-90@P-A**,<sup>50</sup> **CuAl-LDH**<sup>26</sup>). Partly reproduced from ref. 23–26, 50, 51 with permission from Wiley, ACS and Elsevier.

(20% cell viability, 10  $\mu\text{M}$  substrates, MCF-7 cells). This study was extended to an *in vivo* animal model in *C. Elegans* showing full biocompatibility of the catalyst over 15 days as well as fluorescence activation due to the catalytic activity of the Cu-MOF.

Another application of the MOF-catalyzed CuAAC approach was shown by Qu in 2021.<sup>24</sup> The group synthesized a bimetallic Zn/Cu MOF that, after uptake by cancer cells in lysosomes with acidic microenvironments, could release copper ions for the catalysis of the CuAAC click reaction. The acidic release properties were obtained from the zeolitic imidazolate framework-8 (ZIF-8) they employed as delivery vehicle. The MOF successfully

promoted the CuAAC click reaction *in cellulo* to generate a resveratrol analogue (**3**) resulting in reduced cell viability (80%, 100  $\mu\text{M}$  precursors, MCF-7 cells). This strategy was combined with the delivery of a human early growth response-1 (EGR-1) targeted DNAzyme with the corresponding Zn(II) cofactor, targeting metastasis-associated oncogenes to prevent proliferation and metastasis of the cancer cells. This chemotherapy–gene therapy nanoplateform (**DNAzyme@Cu/ZIF-8**) was reported to exert low cytotoxicity (up to 40  $\mu\text{g mL}^{-1}$ ), good cellular uptake, and good synergistic anticancer effects *in vitro* (54% cell death, 75% cell proliferation inhibition). In an animal mice study the MOF showed tumor targetability due to enhanced permeability



and retention (EPR) effect, and excellent tumor growth and metastasis inhibition upon intracellular synthesis of 3. The synergistic effect was clearly noticeable as the control experiments using only one of the two effective pathways showed significantly higher tumor growth and metastasis, indicating the effectiveness of the combined therapy method.

A third application of MOFs towards intracellular drug synthesis was presented by Qu in 2024.<sup>25</sup> In this approach, the ZIF-8 MOF did not deliver exogenous copper atoms, but rather utilized endogenous copper to promote the CuAAC reaction. The amino-functionalized ZIF-8 MOF was covalently conjugated with a *cis*-platin prodrug (Pt(iv)) and modified with folic acid (FA) molecules for cancer cell targeting. The obtained ZIF-8-Pt(iv)-FA (**ZPF**) functioned as a Cu chaperone mimic, binding copper ions and transporting them to cancer cells through FA receptor-mediated endocytosis followed by acid induced release. The Pt(iv) prodrug was reduced *in cellulo* to Pt(II) by upregulated GSH, becoming functional inhibitors in the native copper ion transfer pathway, resulting in copper accumulation in the cancer cells. The **ZPF** was shown to be able to catalyze the CuAAC promoted formation of once again a resveratrol analogue using its endogenous copper accumulative properties, resulting in a significant apoptotic ratio of cancer cells *in vitro* (84%, B16F10 cells). An *in vivo* animal study on mice showed that the **ZPF** had good tumor targeting abilities, as well as significant mice survival rate promotion and cancer cell apoptosis and tissue damaging properties due to intracellular synthesis of 3.

This example was not the first using endogenous copper for the *in situ* CuAAC promoted formation of drugs. In 2019, the group already demonstrated the targeted synthesis of Cu-chelators using neurodegenerative Alzheimer's Disease (AD) related Cu accumulation in A $\beta$ -plaques.<sup>51</sup> After targeted delivery of the prodrug using H<sub>2</sub>O<sub>2</sub>-responsive mesoporous silica nanoparticles (**MSN-IgG**), the prodrug could be transformed into efficient Cu-chelators *via* CuAAC using endogenous copper. The Cu-chelators could extract Cu from A $\beta$ -Cu aggregates and subsequently disassemble them, suppressing A $\beta$ -mediated paralysis and restore locomotive function in an AD model *C. elegans*. Another study by Qu in 2023 utilizing endogenous copper, reported a MOF catalysis system which could be described as a 'DIY' package for self-destruction of cancer cells.<sup>50</sup> The MOF ZIF-90 nanoparticle was functionalized with cancer cell ATP overexpressed targeted aptamers (**ZIF-90@P-A**). Upon endocytosis, a resveratrol derivative prodrug is released, together with the reducing agent sodium ascorbate to boost intracellular Cu(II) concentrations *via* reduction of Cu(II). The boosted Cu(II) could subsequently promote the CuAAC promoted formation of the resveratrol derivative 3. Its efficacy was shown in an animal mice study, significantly inhibiting tumor growth without exerting any side effects towards major organs. These examples show that using endogenous copper towards the *in situ* drug synthesis *via* CuAAC reaction is a promising strategy.

Comparable to the approach of using MOFs or inorganic nanoparticles is the approach presented by Chen in 2023.<sup>26</sup>

The group created a copper-aluminum layered double hydroxide (**CuAl-LDH**) nanosheet as a nanocatalyst for targeted *in situ* CuAAC drug synthesis for tumor therapy. Where many other Cu(II) promoted strategies rely on the *in vivo* reduction of Cu(II) with sodium ascorbate, Qu utilizes the upregulation of glutathione (GSH) in tumor microenvironments (TMEs) to reduce the **CuAl-LDH** Cu(II) to the catalytically active Cu(II).

Additionally, the Cu(II) atoms could not only promote the CuAAC formation of a resveratrol analogue 3 *in vitro* and *in vivo*, it also showed cytotoxic effects through the generation of radical oxygen species (ROS) from increased hydrogen peroxide (H<sub>2</sub>O<sub>2</sub>) levels found in tumor microenvironments (TMEs). Although not explicitly stated, it is assumed that the nanosheets have passive tumor targeting abilities evident from the animal mice study showing significant tumor growth reduction as well as no observed tissue damage to major organs.

**2.1.3 DNA-based nanoparticles.** A different approach towards the *in cellulo* catalysis of the CuAAC reaction is the application of DNA-templated copper nanoparticles. In 2022, Qu published two papers on this topic both showing excellent *in vivo* tumor targeting and therapy efficacy (Fig. 4).<sup>27,52</sup> In the first paper DNA-based nanocatalyst (**DNA-Cu-NP**) was reported consisting of three parts: a poly-thymine (polyT) sequence serving as a template for copper nanoparticle deposition, a DNA aptamer with targeting abilities towards the adenocarcinoma cell overexpressed Mucin1 (MUC1) receptor, and a fifteen base DNA linker connecting the two parts together. They found a 30 base polyT templated Cu-NP to yield the highest conversion rates, converting 90% of substrate within 60 min in an *in vial* fluorescence study.

The aptamer targeting approach was tested with two different aptamers which both showed excellent specific cancer cell type selectivity. The **DNA-Cu-NP** could readily promote the CuAAC click generation of resveratrol analogues *in cellulo* and *in vivo*, resulting in good to excellent tumor inhibitory effects. In the second paper the same DNA-templated Cu-NP approach was employed, however this time with an additional functionality. Instead of an aptamer used for targeting only, a hemin loaded peroxidase-mimicking DNAzyme aptamer was employed with retained cancer cell targeting ability (**DNAzyme-Cu-NP**). This was again linked to a polyT sequence functionalized with a Cu-NP. After targeted internalization in cancer cells, the DNAzyme aptamer part of the system could produce ROS using the high local H<sub>2</sub>O<sub>2</sub> concentration in cancer cells. These active radical species could then oxidize the Cu-NP Cu(0) to Cu(II), enhancing its catalytic activity and enabling the *in situ* CuAAC generation of the anticancer resveratrol analogue. The resveratrol analogue and the cancer-killing ROS together, result in an effective synergistic anti-tumor combination.

## 2.2 Palladium catalysis

Palladium catalysts are extremely versatile in organic chemistry due to their capability of catalyzing various C-C bond forming cross-couplings leading to the awarding of the Nobel prize in chemistry in 2010. Examples include the Heck reaction, Buchwald-Hartwig reaction, Sonogashira coupling, and Suzuki-Miyaura coupling (Fig. 5).<sup>53</sup> These reactions utilize substrates



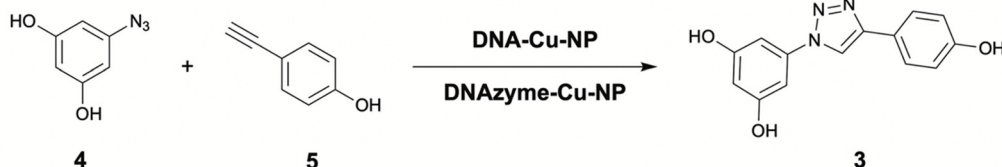
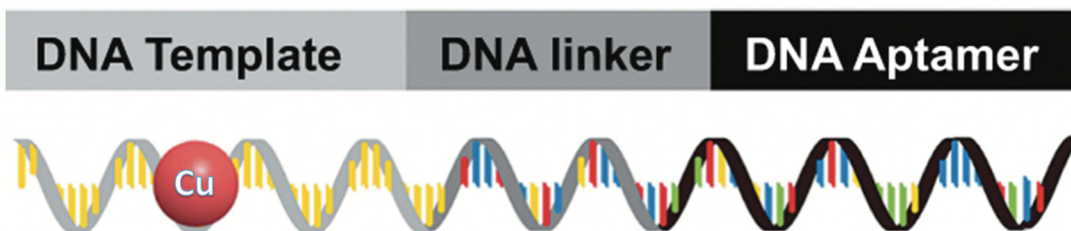
**A****B**

Fig. 4 (A) Formation of resveratrol analogue **3** from precursors **4** and **5** via CuAAC and corresponding DNA-based catalysts **DNA-Cu-NP**<sup>52</sup> and **DNAzyme-Cu-NP**.<sup>27</sup> (B) Schematic representation of the DNA-based catalysts. Secondary structures are not shown. Partly reproduced from ref. 52 with permission from Springer.

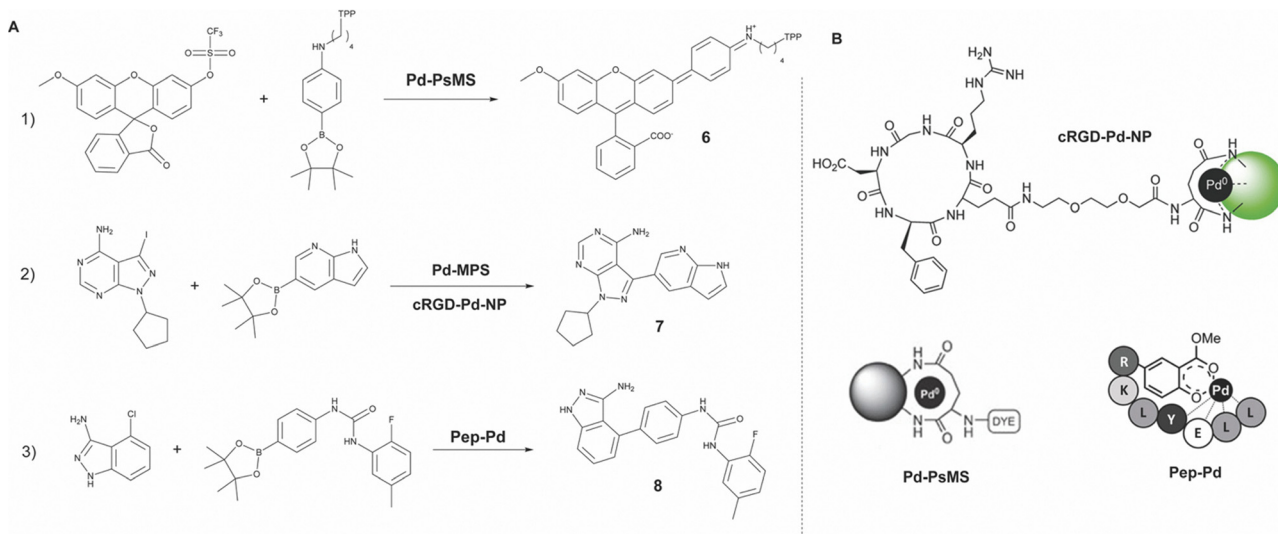


Fig. 5 Overview of reported Pd catalyzed Suzuki–Miyaura cross-couplings (SMcc) (A) and respective Pd functionalized macromolecular platforms (B). (1) Formation of rhodamine 110 derivative (**6**) via **Pd-PsMS** catalyzed SMcc,<sup>28</sup> (2) formation of cytotoxic agent PP-121 (**7**) via **Pd-MPS**<sup>29</sup> and **cRGD-Pd-NP**<sup>55</sup> catalyzed SMcc, (3) formation of Linifanib (**8**) via **Pep-Pd** catalyzed SMcc.<sup>56</sup> Partly reproduced from ref. 28, 55 and 56 with permission from Wiley, ACS and Springer.

that are not commonly found in nature and therefore serve as an excellent recipe for bioorthogonal chemistry. Palladium exerts low toxicity unlike other transition metals such as copper and additionally can withstand oxygen and moisture. However, palladium catalysts have been shown to be poorly endocytosed, sometimes have low catalytic ability in water, and are readily inhibited by thiols such as glutathione (GSH), making their incorporation into nano-structured delivery tools essential.<sup>54</sup>

The first example of *in cellulo* Pd mediated SMcc reaction was presented by Bradley in 2011.<sup>28</sup> The group synthesized an amino-functionalized polystyrene microsphere ( $\sim 500$  nm) and

doped them with Pd(0) nanoparticles (**Pd-PsMS**), locked in place through extensive crosslinking of the amine moieties. The microspheres showed cellular uptake (HeLa cells) and good biological compatibility with low cytotoxicity ( $< 9\%$  cell death, 48 h,  $0.38 \times 10^{10}$  beads per mL). The microspheres capability for catalyzing the SMcc reaction was shown in a fluorescence study *via the in cellulo* synthesis of the fluorescent dye rhodamine 110 derivative (**6**) from triflate and boronate precursors. After 48 h clear fluorescence was observed around mitochondria due to TPP induced mitochondrial targeting of the formed dye.



Continuing this research, in 2016 the Bradley group presented the formation of an anticancer agent in the extracellular media using a similar SMcc strategy.<sup>29</sup> This time the group did not employ endocytosed Pd(0) microspheres, but a large modular polymeric support functionalized with Pd(0) nanoparticles (**Pd-MPS**). This was then used in a cancer cell (PC-3 cells) viability study where cytotoxic agent PP-121 (7) was formed *via* SMcc from iodopyrazole and boronic ester precursors (2 and 10  $\mu$ M respectively) in the extracellular media. This resulted in 50% cell death over 5 days.

In 2017, Bradley and co-workers expanded this research to Pd(0) functionalized microspheres for the intracellular catalysis of a tandem formation of two anticancer drugs *via* different chemistries.<sup>55</sup> Here the original microspheres ( $\sim$  208 nm) were again doped with Pd(0) nanoparticles and afterwards functionalized with cyclic-RGD cancer targeting moieties (**cRGD-Pd-NP**) selective for integrin ( $\alpha_5\beta_3$ )-positive cancer cells.

The cellular uptake was shown to be  $>95\%$  within one hour in integrin-positive human glioblastoma cell line U87-MG as compared to  $<4\%$  in integrin-negative human breast adenocarcinoma cell line MCF-7, indicating good targeting functionality. Afterwards the Pd(0) catalyst was employed in a cell viability study for the simultaneous deprotection of pro-5-fluorouracil (pro5FU) and the SMcc promoted formation of PP-121 (7), both known anticancer drugs. The synergistic effect of the dual therapy strategy was clearly shown with a cell viability as low as 22% over 5 days as compared to the separate strategies (66% and 44% respectively). This strategy has potential but shows relatively slow results as compared to for instance CuAAC strategies (5 days *vs.* 24 h).

A different application of the SMcc reaction in biologically relevant media was presented by Mascareñas in 2018.<sup>30</sup> They employed hollow mesoporous silica nanoshell microspheres functionalized with an inner layer of Pd(0) nanoparticles (**Pd-MSNs**). The SMcc reaction yielded up to 86% conversion of starting materials over 24 h in water and PBS. However, where the depropargylation reaction of this system was successful, the SMcc reaction failed upon the presence of biorelevant thiols and did not proceed in cell lysates or in the presence of Vero cells.

An approach which will be more extensively visited later in this review, is the application of artificial metalloenzymes (ArMs). Palladium, however, has until now not yet been employed in this strategy. An approach closely resembling the ArM strategy, is the generation of metallopeptides as reported by Rappaport in 2023.<sup>56</sup> Rappaport claims these might have a structural advantage over large metalloenzymes regarding delivery, no need for *in situ* assembly, and absence of immunogenicity. A methyl salicylate tagged hydrophilic peptide (LLEYLKR), chosen for its water soluble and hydrophobic pocket containing properties, was functionalized with a Pd(II) complex (**Pep-Pd**), and tested in a fluorescence study for its catalytic abilities towards depropargylation and SMcc reactions in PBS. The SMcc reaction was reported to be less efficient due to insufficient *in situ* reduction to Pd(0), the active catalyst for the SMcc reaction. The cytotoxicity of the metallopeptide was

reported to be negligible up to 400  $\mu$ M. A cell viability study (A549 lung cancer cells) showed that the *in situ* formation of two anticancer drugs (Paclitaxel (PTX) *via* depropargylation, Linifanib (LNF, 8) *via* SMcc) had a large synergistic effect evident from 28% cell viability over 5 days as compared to 67% and 61% of the separate methods. However, in this study the precursors for the SMcc reaction were applied in a 100 $\times$  higher concentration than those of the depropargylation reaction because of the relatively low cytotoxic potency of LNF, rendering the bond-forming reaction less efficient. Although metallopeptides might not clearly fit in the description of 'macromolecular platform', they serve as a powerful example for the implementation of innovative strategies for catalyst shielding and delivery in a bioorthogonal manner.

Besides employing SMcc, other Pd catalyzed bond-forming reactions have been applied in biologically relevant media. An example of this is the application of a Heck coupling reaction as reported by Weissleder in 2017.<sup>31</sup> They identified  $\text{PdCl}_2(\text{TFP})_2$  as an under physiological conditions active catalyst and trapped it into an FDA approved poly(lactic-co-glycolic acid)-polyethylene glycol (PLGA-PEG) scaffold to form nanoparticles (Fig. 6), ultimately providing a Pd-catalyst nanoparticle (**PLGA-PEG-Pd**). Although the Pd-nanoparticle was successfully applied towards *in vivo* prodrug decaging in anti-tumor therapy, the intramolecular Heck coupling reaction has only been applied in an *in cellulo* fluorescence study for the formation of a coumarin derivative.

If a suitable retrosynthetic Heck coupling anticancer compound could be identified, this strategy could be very interesting for further studies towards *in situ* bond-forming drug synthesis.

### 2.3 Ruthenium catalysis

Ruthenium (Ru) has gained significant attention for catalysis in organic chemistry due to its high versatility, catalyzing a wide variety of reactions, such as hydrogenation, hydrogen transfer,

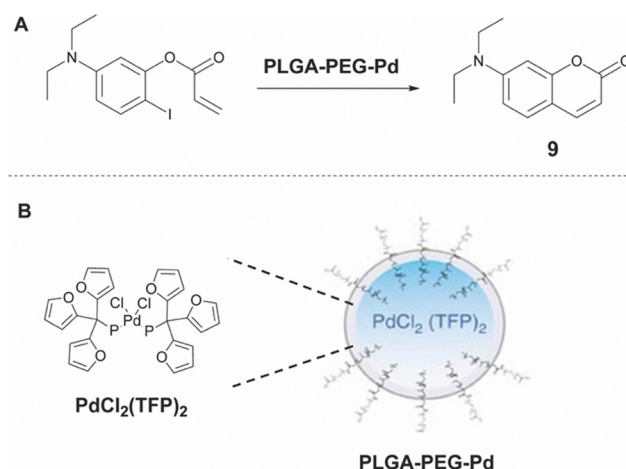


Fig. 6 (A) Formation of coumarin derivative 9 *via* PLGA-PEG-Pd catalyzed Heck coupling. (B) Schematic structure of PLGA-PEG-Pd.<sup>31</sup> Partly reproduced from ref. 31 with permission from Springer.



metathesis, oxidation and cross-coupling reactions.<sup>57</sup> Ru catalyzed metathesis and cross-coupling reactions are both bond-forming reactions, of which Grubbs olefin metathesis is the most famous example. This reaction has been used for different kinds of olefin metathesis such as cross metathesis (CM), ring-closing metathesis (RCM), ring-opening metathesis polymerization (ROMP), enyne metathesis, and cross-coupling metathesis (CMC).<sup>58</sup>

Artificial metalloenzymes (ArMs) are a combination of proteins with organometallic catalysts, anchored through covalent, dative, or supramolecular interactions.<sup>59</sup> Ruthenium complexes are highly toxic,<sup>60</sup> and therefore benefit from being shielded and prevented from leaking by ArMs if applied to *in vivo* catalysis. Embedding the catalysts in a biomacromolecular scaffold, protects the Ru catalyst from inhibition by proteins and metabolites and promotes enzyme-like catalysis.

One of the earliest examples of ruthenium promoted metathesis reactions using the ArM approach was presented by Ward in 2016 (Fig. 7).<sup>32</sup> The group employed biotin-streptavidin technology by anchoring a biotin functionalized second generation Hoveyda–Grubbs Ru catalyst into a streptavidin protein, shielding it from biological inhibition of the catalyst (**SAV-biot-Ru**). They then used and evolved this ArM (**SAV-biot-Ru**) for the bioorthogonal olefin ring-closing metathesis (RCM) reaction. It was shown in a fluorescence study that this system was able to catalyze the RCM reaction forming umbelliferone (**10**) in the periplasm of *Escherichia coli* bacteria. The Ru-ArM was not affected by the glutathione disulfide (GSSG) present here but was inhibited by glutathione (GSH) present in the cytoplasm resulting in reduced catalytic efficiency. Upon saturation mutagenesis optimization screening, an ArM was found with improved *in vitro* and *in vivo* activity towards various substrates (TON: up to 90), outperforming two commercially available metathesis catalysts (second-generation Hoveyda–Grubbs and AquaMet).

Similar to this approach is that presented by Tanaka in 2019, as a continuation on his earlier endeavors focusing on *in vivo* gold catalysis in 2017 (*vide infra*).<sup>33</sup> The group developed a human serum albumin (HSA)-based ArM that could protect the

Ru RCM catalytic ability of a second generation Hoveyda–Grubbs Ruthenium catalyst in the presence of up to 20 mM GSH, rendering it biocompatible. The Ru catalyst was anchored in the HSA using a coumarin moiety attached with a PEG spacer. To extend this system towards *in vivo* anti-cancer therapy, a glycosylated albumin targeting strategy was employed. After functionalization of the Ru-ArM with  $\alpha$ (2,3)-linked sialic acid terminated *N*-glycans (**Ru-GArM**), good targetability of cancer cells (SW620 > HeLa > A549) was shown in an RCM activated fluorescence study. To assess the possibility of prodrug therapy, the **Ru-GArM** was employed in a cell cytotoxicity study with the SMcc prodrug activation of the anti-cancer drug umbelliprenin (**11**). This resulted in cell growth inhibition of up to >95% (32  $\mu$ M precursor, 25  $\mu$ M **Ru-GArM**), showing significant difference compared to the non-glycosylated ArM ( $\sim$ 10% cell growth inhibition), indicating the importance of targeted therapy strategies.

In a continuation on these studies, Tanaka focused on a concept which he called ‘retrosynthetic prodrug design’, taking existing drugs and retrosynthetically disassembling them for prodrug design, focusing on optimization of the prodrug rather than the optimization of the biocatalyst.<sup>18</sup> The key advantage of retrosynthetic prodrug design is the large increase in possibilities towards the optimization of reactivity, catalytic efficiency, bioavailability and difference in bioactivity between the prodrug and drug resulting in higher side effect suppression.

Using this concept, rather than improving the biocatalyst (**Ru-GArM**), it was attempted to optimize the prodrug, improving cascade reactivity (*via* enhanced aromatization), activity with the biocatalyst, hydrolytic stability in blood, and reducing intrinsic prodrug bioactivity. As previously seen, it was found that substrate hydrophobicity played an important role in the substrate/ArM interaction. Multiple CA4 derivatives were identified as suitable retrosynthetic prodrug candidates. A prodrug designed with a citronellate moiety was found to exert low tubulin affinity compared to the drug ( $-1.15$  vs.  $-9.2$  kcal mol $^{-1}$ ), favorably increasing the bioactivity difference. However, out of the tested substrates a prodrug containing a pivalate moiety (**12**) instead, showed the highest catalytic conversion rate

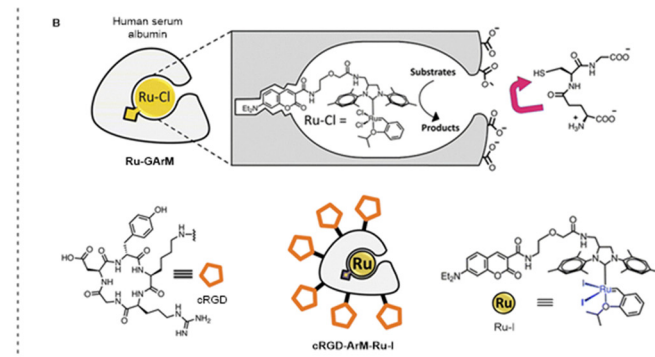
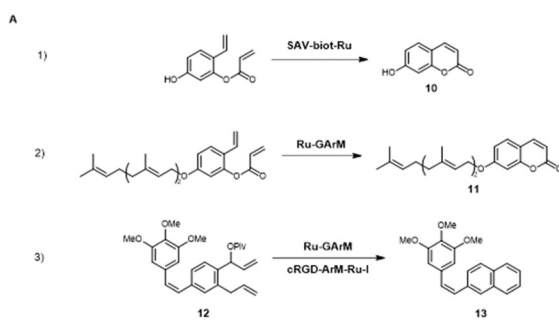


Fig. 7 Overview of reported ruthenium catalyzed metathesis reactions (A) and respective ruthenium artificial metalloenzymes (Ru ArMs) (B). (1) Formation of umbelliferone (**10**) via **SAV-biot-Ru** catalyzed ring closing metathesis (RCM),<sup>32</sup> (2) formation of umbelliprenin (**11**) via **Ru-GArM** catalyzed RCM,<sup>33</sup> (3) formation of pivalate combretastatin A4 (**13**) from precursor **12** via **Ru-GArM**<sup>33</sup> and **cRGD-ArM-Ru-I**<sup>61</sup> catalyzed RCM. Partly reproduced from ref. 33 and 61 with permission from RSC and Springer.



( $k_{\text{cat}}/K_M = 457.9$  vs.  $84.1$  &  $108.7 \text{ M}^{-1} \text{ s}^{-1}$ ) as well as largest hydrolytic stability in blood (9.8% vs. 22.3 & 31.5% hydrolysis, 2 h), and was therefore selected as the most suitable candidate. Upon cytostatic analysis potential in a HeLa cell line, the pivalate prodrug/Ru-GarM combination proved highly effective, achieving a 50% cell growth reduction already at  $4 \mu\text{M}$  (12) and  $130 \text{ nM}$  (Ru-GarM). Upon conducting an *in vivo* mice study *via* intravenous (i.v.) injection, the system was shown to exert a significant although not complete tumor growth inhibition property.

Since the prodrug/Ru-GarM system was previously injected intraperitoneally instead of intravenously, the difference between *in vitro* and *in vivo* application, was attributed to blood (cells and metabolites) induced quenching of the reaction.

To combat the blood induced quenching of the Ru-ArM promoted RCM, Tanaka improved the Ru-ArM in a recent study in 2023.<sup>61</sup> After exchanging the Ru-Cl anchored catalyst for a Ru-I catalyst, the yield of a model RCM reaction in blood increased significantly (88% vs. 19% over 3 h) at a catalyst loading of the albumin of only 2.5%. It even continued to show RCM yields (21%) after 24 h incubation in blood. Besides RCM it was shown that the newly obtained Ru-I-ArM was also able to efficiently catalyze enyne RCM and olefin cross metathesis in blood environment. After functionalization of the Ru-I-ArM with a cyclic-Arg-Gly-Asp (cRGD) pentapeptide (cRGD-ArM-Ru-I), selective for cancer cell integrin overexpression, an *in vivo* tumor growth inhibition study with i.v. administration was performed on SW620-xenografted mice. At a loading of only  $20\text{--}40 \text{ mg kg}^{-1}$  of the cRGD-ArM-Ru-I, a significant dose dependent tumor growth inhibition effect was observed due to formation of pivalate combretastatin A4 (13), whereas none was observed whatsoever using the cRGD-ArM-Ru-Cl, indicating the high efficiency and blood stability of the new Ru-ArM. Additionally, the cRGD targeting efficacy was clearly noticeable as the system exerted a higher tumor growth suppression than the direct administration of the post RCM CA4 drug.

#### 2.4 Gold catalysis

Traditionally, gold (Au) was considered inert and inactive in general chemistry. However, in modern-day chemistry, Au nanoparticles and complexes are highly effective catalysts due to their electronic properties and ability to activate a wide range of substrates. Gold catalysis is used for a diverse array of transformations including hydroamination, hydroarylation, hydroalkoxylation, and C–H activation. The most common pattern in Au-catalysis is the activation of alkynes allenes and olefins for nucleophilic attack, efficiently creating carbon–heteroatom and carbon–carbon bonds. Au-catalysts tolerate both oxygen, water, and acidic environment and are compared to other transition metal catalysts for similar reactions significantly more active.<sup>62</sup>

Au-catalysis in biological systems suffers from side reactivity with biomolecules and intracellular reducing agents, such as GSH, which inhibit the catalytic activity. To overcome this, various strategies have been employed to protect and enhance the catalytic activity in intracellular environments. Additionally,

since Au activates substrates for nucleophilic attack, intramolecular cyclization reactions are preferred over intermolecular reactions for the purpose of intracellular drug synthesis because of the presence of many nucleophiles in biological environments.<sup>63</sup>

The first application of gold mediated intracellular catalysis using an ArM approach, was reported by Tanaka in 2017, a preliminary study to Tanaka's Ru-ArM studies previously described (*vide supra*).<sup>34</sup> The group developed a glycosylated albumin Au(III) ArM, which enabled *in vivo* localized propargyl ester amidation, resulting in organ specific fluorescence in mice studies. The Au-GarM consisted of a coumarin functionalized cyclometallated Au(III) catalyst anchored inside the organ targeting glycosylated albumin. Upon localized Au-activation of the fluorescent probe, surface amino groups could ligate to it resulting in fluorescence accumulation.

In a continued study in 2021, Tanaka applied the albumin Au-ArM approach towards the *in situ* synthesis of anticancer phenanthridinium derivatives *via* Au(I) promoted hydroamination (Fig. 8).<sup>64</sup> The group identified a new carbene functionalized Au(I)-Cl catalyst that performed the hydroamination reaction on various substrates with high TONs ( $>200$ ) and good yields (50–99%, 3 h). The unmodified Au-catalyst was applied in a cell viability study (A549 cells) to form a phenanthridinium derivative (17) *via* Au-catalyzed hydroamination. This resulted in a decrease in cell growth of  $>50\%$  already at a prodrug and catalyst concentration of 8 and  $2.5 \mu\text{M}$  respectively (4 d). To be able to employ this system *in vivo* and shield it from biological GSH, the catalyst was anchored in an albumin scaffold, forming a new Au-ArM. This Au-ArM resulted in sustained catalytic activity even upon addition of  $1200 \mu\text{M}$  GSH (TON  $> 100$ ). The new Au-ArM was applied in a new cell viability study, resulting in even better results compared to the unmodified Au-catalyst (50% cell growth inhibition at  $0.63 \mu\text{M}$  catalyst, 4 d).

In 2022, Tanaka and Yokoshima demonstrated that the same albumin-Au-ArM with SW620 cancer cell-targeted glycosylation (Au-GarM) could also be employed for the synthesis of dehydro-pyrrolizidine alkaloids (DHPs, 18) *via* a gold catalyzed hydroamination cyclization of the precursor molecule.<sup>35</sup> In a targeted cancer cell viability study (HeLa, PC3, A549, SW620

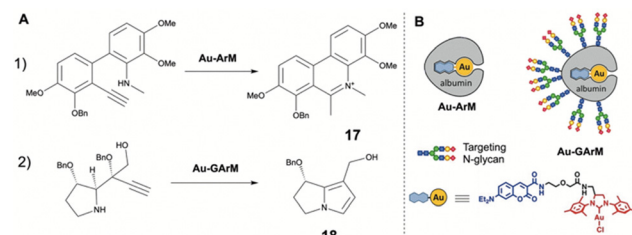


Fig. 8 Overview of reported gold catalyzed reactions (A) and respective albumin based gold artificial metalloenzymes (Au-ArMs) (B). (1) Formation of phenanthridinium derivative (17) *via* Au-ArM catalyzed hydroamination.<sup>64</sup> (2) Formation of dehydropyrrolizidine alkaloid 18 *via* Au-GarM catalyzed hydroamination.<sup>35</sup> Partly reproduced from ref. 35 with permission from Wiley.



cells), a cell growth inhibition of  $>50\%$  was achieved with prodrug and **Au-GarM** concentrations of 64 and  $2.5\text{ }\mu\text{M}$  respectively. These albumin-based targeted **Au-GarM** approaches shows great potential for *in vivo* anti-tumor therapy strategies.

## 2.5 Iridium catalysis

Iridium (Ir) is a versatile transition metal for catalysis in organic chemistry. Due to its wide range of oxidation states ( $-3$  to  $+9$ ), Ir exerts various unique properties for a broad area of applications. It is known to catalyze reactions such as cycloadditions, allylic substitutions, C–H functionalization, hydrogenation, hydrogen transfers and photo-redox catalysis.<sup>65</sup> Iridium's low intrinsic cytotoxicity and its high tolerance for water, oxygen and bio-additives indicate biocompatibility.<sup>66</sup> However, despite its versatility, it is still highly underrepresented in bioorthogonal chemistry when compared to metals such as palladium and copper.

The difficulty of the translation of iridium chemistry into biological systems is the general insolubility of iridium compounds as well as catalytic inhibition due to metabolites and enzymes that bind iridium. A few examples of *in vivo* Ir-catalyzed reactions have been reported although limited to hydrogen transfer, uncaging and photo-redox reactions.<sup>66–68</sup>

Iridium catalyzed bond-forming reactions have scarcely been used towards potential intracellular catalysis. One known example was shown by Hartwig in 2021 and elaborated upon in 2022 (Fig. 9).<sup>69,70</sup> The group reported an iridium porphyrin cofactor (**Ir-Por**) that complexes *in cellulo* (*E. coli*) with a cytochrome P119 to form an iridium ArM (**Ir-Por-ArM**) that catalyzes stereoselective carbene insertions into benzylic C–H bonds. Although these studies are focused on synthetic biology, they display the potential for Ir-catalyzed reactions *in vivo*.

Other examples of cyclopropanation through cofactor insertion in native and engineered proteins have been reported for iridium<sup>71</sup> and iron (heme cofactor,<sup>72–79</sup>) However, since these studies are focused on synthetic biology and not *in vivo*

catalyzed drug formation, they are considered outside of the scope of this review and will not be further discussed.

## 2.6 Rhodium catalysis

Rhodium (Rh) catalysis has been around in organic chemistry a little over 25 years, significantly shorter than other transition metal catalysis such as Pd-catalysis.<sup>80</sup> With respect to C–C bond forming reactions, however, rhodium has displayed interesting catalysis, coupling common reagents in ways not demonstrated before by other transition metal catalysts, enriching the possibilities within organic chemistry. Examples include cycloadditions, hydroacylation reactions, and allylic functionalizations.<sup>80</sup> Rhodium catalysts also show great potential for environmentally benign reactions since water can often be used as cosolvent or sole solvent. However, *in vivo* applications are limited due to rhodium's high toxicity and carcinogenicity due to its DNA binding preferences and are therefore still highly underrepresented in this field.<sup>81</sup>

The first and, to the best of the authors knowledge, only report of *in vivo* Rh-catalysis was presented by Ward in 2018<sup>82</sup>. The group employed biotin-streptavidin technology to develop a dirhodium ArM (**SAV-biot-Rh**) capable of catalyzing carbene transfer reactions inside living bacteria. With this **SAV-biot-Rh** it was possible to promote intermolecular cyclopropanation (diazo + olefin precursors) and C–H carbene insertion reactions. Although carbene transfer reactions catalyzed by dirhodium complexes prove to be biocompatible, the application towards *in vivo* drug synthesis might be difficult. Diazo compounds have been shown to be useful tools in chemical biology,<sup>83</sup> but many reactive components found in biological environments serve as good substrates for C–H insertion (e.g. amino acids<sup>84</sup>). An interesting approach to overcome this in future studies, might be the design of an intramolecular prodrug scaffold.

## 3. Multimodality: the need for macromolecular platforms

Site and time specific (spatiotemporal) control over *in situ* synthesis can be obtained through external triggers. By using drug delivery tools including polymeric or biomacromolecular nanocarrier both active and passive targeted drug delivery have been realized. In comparison to non-specific therapeutic treatments, prodrug activation strategies give promising results and thereby greatly reduce off-target effects. However, because these strategies are based on endogenous factors which lack perfect selectivity, non-specific delivery or activation might still occur leading to unwanted toxicity. One approach to overcome this challenge is the addition of an exogenous trigger responsive functionalization. Compared to traditional small molecule-based drug delivery platforms, polymeric nanomedicines offer the advantage of multimodality, allowing the incorporation of additional functions – often without synthetically altering the bioactive payload. Exogenous triggers such as light, magnetic fields, heat, or ultrasound, can be applied with high precision

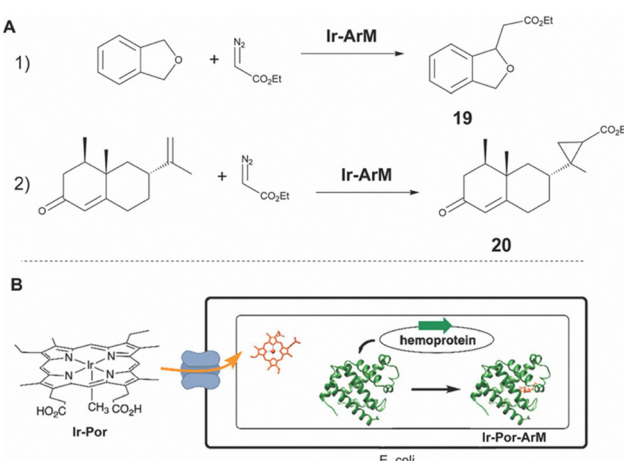


Fig. 9 (A) Formation of **19** and **20** via intracellular **Ir-Por-ArM** catalyzed carbene insertion reactions. (B) Intracellular formation of **Ir-Por-ArM** from **Ir-Por** cofactor and hemoprotein cytochrome P119.<sup>69,70</sup> Partly reproduced<sup>69</sup> with permission from ACS.



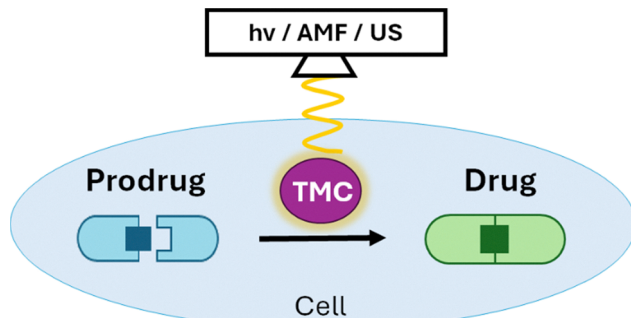


Fig. 10 Bond-forming *in situ* prodrug activation through external trigger-controlled catalysis.

and – importantly – spatiotemporal control to selectively activate drug formation at the desired location, further preventing off-target effects (Fig. 10).<sup>85,86</sup>

In this section representative examples are given of exogenous control applied to *in situ* bond-forming drug synthesis, mainly showing its potential and efficacy. Throughout the given examples it will become clear that the implementation of nanostructures is vital to the incorporation of secondary functionalities, from incorporation of responsive materials to shielding of catalytic functionality and accommodation of nano-reactors. For further reading on stimuli-responsive systems, we refer to specialized reviews.<sup>87–90</sup>

### 3.1 Light triggered *in situ* catalysis

The application of light is an effective and easy way of administering energy to a system, activating and accelerating chemical reactions.<sup>91</sup> Light of different wavelengths carry different energies (small wavelengths have high energy) and have different effects on biological tissues. UV-light (<400 nm) has high energy, can cause severe photo-damage to tissue, and has very low tissue penetration depth making it invaluable for many *in vivo* applications. Visible light (400–700 nm) and near-infrared light (NIR-I: 700–900 nm, NIR-II: 900–2000 nm) cause significantly less photodamage and have higher penetration depths up to 10 cm.<sup>92,93</sup> Even though light is already extensively used in multimodular nanomedicine strategies for drug delivery, (uncaging) prodrug activation, and targeting,<sup>94</sup> its application towards *in situ* drug synthesis is novel and underexplored.

A light-promoted palladium catalyzed SMcc approach for *in situ* synthesis was reported by Qu as early as 2018 (Fig. 11).<sup>95</sup> The group presented a microporous silica–Pd(0) nanoparticle functionalized with azobenzene and shielded with  $\beta$ -cyclodextrin (CD) through host–guest interactions (CASP). Here, usage of the microporous silica nanoparticle is vital for the accommodation of the light responsive azobenzene. The CD shielding of the Pd-nanoparticles caused catalyst inhibition through obstruction of the catalytic sites. However, upon illumination with UV-light, isomerization of the azobenzene induced release of the CD blocker, restoring the catalytic function of the Pd. The CASP showed good cellular uptake, low cytotoxicity, also in combination with low-dose UV-irradiation. CASP displayed good intracellular light activated

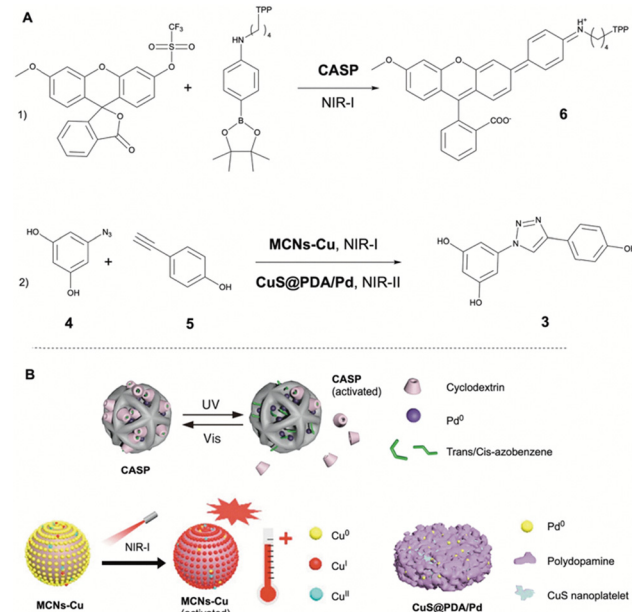


Fig. 11 Overview of reported catalyzed reactions (A) and respective light activated catalysts/catalytic systems (B). (1) Formation of rhodamine 110 derivative (**6**) via **CASP** catalyzed Suzuki–Miyaura cross-coupling after activation with NIR-I light.<sup>95</sup> (2) Formation of resveratrol derivative **3** via CuAAC catalyzed by **MCNs-Cu** after NIR-I light activation,<sup>91</sup> and **CuS@PDA/Pd** after NIR-II light activation.<sup>96</sup> Partly reproduced from ref. 91, 95 and 96 with permission from ACS and Springer.

catalytic activity in a fluorescence study through the formation of rhodamine 110 (**6**) via cleavage and a rhodamine derivative via SMcc reaction. This study presents a promising approach towards light-activated bioorthogonal catalysis. However, UV-light is not the ideal choice for *in vivo* applications because of its intrinsic biological interference.

The first copper based light-promoted *in vitro* and *in vivo* catalysis approach was presented by Qu in 2020.<sup>91</sup> For this purpose, the group constructed a mesoporous carbon nanosphere functionalized with copper nanoparticles (**MCNs-Cu**). Upon irradiation with near infrared light (NIR,  $\lambda_{\text{em}} = 808 \text{ nm}$ ) the carbon nanostructure heats up (again showing nanostructure necessity) and the **MCNs-Cu** can form reactive oxygen species (ROS) which were able to convert Cu(0) into Cu<sup>1</sup>. Additionally, the **MCNs-Cu** could convert the NIR irradiation efficiently into heat ( $\eta = 51\%$ ), increasing local temperature and accelerating the catalytic process significantly (5-fold fluorescence increase *in vitro*). In a cell viability study, only small effects (85% cell viability) were observed for NIR irradiation of intracellular **MCNs-Cu** (up to  $100 \mu\text{g mL}^{-1}$ ) at a power density of  $1.0 \text{ W cm}^{-2}$  for 5 minutes. Addition of resveratrol derivative precursors ( $10 \mu\text{M}$ ) resulted in significantly higher cell death (75%) with NIR irradiation than without (40%), which was attributed to the more efficient *in situ* resveratrol (**3**) formation as well as the increase in oxidative stress. After toxicological analysis, the system was applied *in vivo* in a mice tumor model, showing great antitumor potential with minimal side effects over 14 days.

To further improve on their previous strategy, Qu reported a new approach for light promoted antitumor therapy in 2022<sup>96</sup>. Instead of using NIR-I light ( $\lambda_{\text{em}} = 650\text{--}950\text{ nm}$ ), they employed NIR-II light ( $\lambda_{\text{em}} = 1000\text{--}1700\text{ nm}$ ) for its deeper tissue penetration and higher maximum permissible exposure.

The 1064 nm laser was used to catalyze CuAAC as well as Pd decaging reactions *via* activation of functionalized nanocatalysts. The nanocatalysts consisted of CuS nanoplatelets (nanostructure with secondary functionality) coated with polydopamine and functionalized with Pd nanoparticles (**CuS@PDA/Pd**). The catalyst displayed great photothermal properties increasing temperature to 52 °C within 10 minutes of irradiation ( $\eta = 58\%$ ), thereby increasing the Pd catalyzed decaging rate by 6-fold as determined by fluorescence. However, the CuAAC reaction showed no acceleration upon NIR-II irradiation. In a cell viability study, it was shown that the NIR-II light was indeed less invasive than the NIR-I light reported in the previous study (only 82% cell viability over 30 min, 1.0 W cm<sup>-2</sup>). Also, the combined anticancer strategy (Pd decaging and CuAAC) of *in situ* formation of 5FU and a resveratrol derivative (**3**) upon NIR-II irradiation, showed good synergistic effects as compared to the separate strategies (cell viability 27% vs. 54% and 43%, 3 d). In an *in vivo* mice study, the system showed highest efficacy using the dual therapy strategy with NIR-II light irradiation compared to the separate strategies or the dual strategies with NIR-I light irradiation. This indicates the utility of dual drug anticancer therapies as well as the applicability of NIR-II irradiation in *in vivo* synthesis. However, it remains a question whether NIR-II could also be applied to deep tissue therapy.

### 3.2 Magnetic field induced catalysis

The application of magnetic fields as an external trigger for *in situ* drug synthesis has great intrinsic potential. Because of the deep tissue penetration, controllability, and low energy transfer to the bioenvironment, magnetic fields provide a great option for energy stimulation. This has been shown by Lee in 2020, who employed a silica-confined magnetothermia-induced nanoreactor for intracellular Pd catalyzed carbocyclization (Fig. 12).<sup>97</sup> The nanoreactors (**MAG-NER**) were created through amino-silica coating of iron-oxide nanoparticles, followed by hollowing of the silicon shell through hydrolysis and subsequent Pd nanoparticle growth on the iron-oxide core. Notably, the iron-oxide core functions as an alternating magnetic field (AMF)-nanoheater, transferring energy to the Pd nanoparticle activating it towards catalysis. The silicon shell nanoparticle accommodates the nanoreactor shielding it from deactivation. The **MAG-NER** showed high catalytic ability in various biologically relevant media (55–70% yield, 1 h, PBS, BSA, DMEM, cell lysates) upon AMF induction. The cellular uptake of the nanoreactor was shown to be high with 65% after 4 h, and the cytotoxicity low (89% cell viability, 500 µg mL<sup>-1</sup>, 48 h) even under AMF exposure (90% cell viability, 30 min). Finally, in a fluorescence experiment, procoumarin was converted into coumarin derivative (**16**) *via* Pd promoted carbocyclization reaction, resulting in clear strong fluorescence after AMF

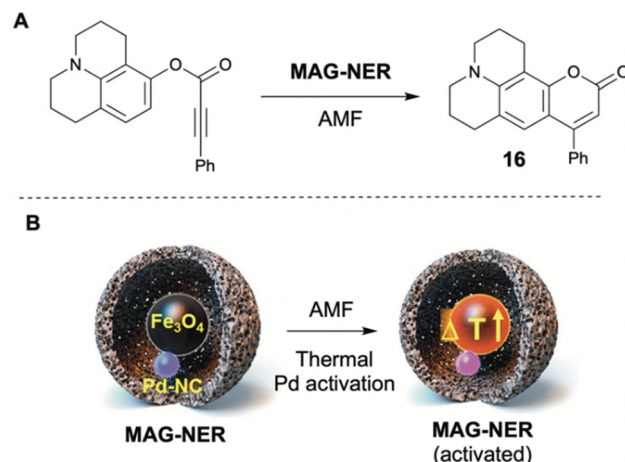


Fig. 12 (A) Formation of coumarin derivative **16** via **MAG-NER** catalyzed carbocyclization after catalyst activation using an alternating magnetic field (AMF). (B) Schematic representation of **MAG-NER** and its AMF activation mechanism.<sup>97</sup> Partly reproduced from ref. 97 with permission from ACS.

application for 30 minutes, compared to no fluorescence without AMF application. This study clearly shows the excellent applicability of magnetism activated *in situ* synthesis of molecules, showing great potential for future *in vivo* studies.

### 3.3 Ultrasound-triggered catalysis

An external trigger that has not often been combined with *in situ* catalyst activation, is the use of ultrasound (US). US, just as magnetic fields, is intrinsically biocompatible and can be applied with high spatiotemporal control. In 2022, Chen reported a copper based polymeric nanocomplex (**Cu@PAA-NC**), able to achieve US promoted CuAAC catalysis (Fig. 13).<sup>98</sup> *Via* exogenous ultrasound irradiation the interconversion between CuAAC inactive Cu(II) and the CuAAC active Cu(I) in the **Cu@PAA-NC** could be reversely regulated.

The reverse transformation to Cu(II) was caused by oxygen or H<sub>2</sub>O<sub>2</sub> exposure, generating ROS in the process. The **Cu@PAA-NC**

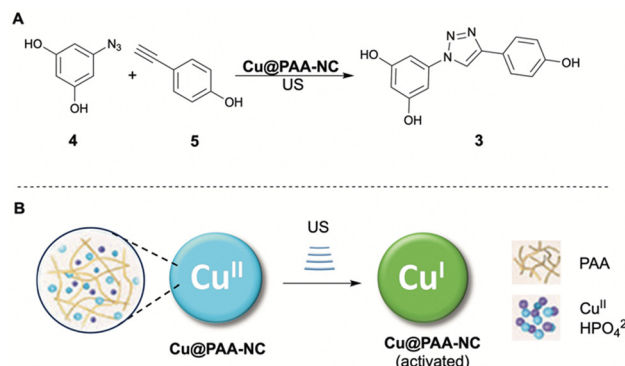


Fig. 13 (A) Formation of resveratrol analogue **3** via **Cu@PAA-NC** catalyzed CuAAC after catalyst activation with ultrasound (US). (B) Schematic representation of **Cu@PAA-NC** and its activation mechanism using US.<sup>98</sup> Partly reproduced from ref. 98 with permission from Wiley.



proved to successfully catalyze the CuAAC reaction under US irradiation *in cellulo*, forming a triazole fluorophore.

In a cell viability study a resveratrol derivative (3) was formed *in situ* with high yield (84%, 12 h) resulting in 36.8% cell viability (80  $\mu\text{g mL}^{-1}$  Cu-NC), indicating Cu-NC to act as an effective sonosensitizer. In an *in vivo* mice study, the Cu@PAA-NC displayed fast passive tumor accumulation, efficient renal metabolism mediated clearance, and no toxicity effects. Additionally, the system displayed excellent synergistic tumor growth suppression in 4T1 and B16-F10 melanoma models: 66% and 68% suppression with Cu@PAA-NC + US irradiation only (ROS induced cell death), and 79% and 94% suppression with Cu@PAA-NC + US irradiation + resveratrol derivative precursors respectively, without any observed off-target effects. This highly effective novel method of *in situ* catalyst activation thus shows great potential for tumor therapy with high spatiotemporal control.

## 4. Modes of application

So far, it has been demonstrated that there are a lot of diverse strategies for bioorthogonal *in situ* bond-forming synthesis of various molecules, fluorophores, and drugs, ranging from *in vial* to *in vivo* examples. However, towards clinical applications, targeted delivery of the therapeutic system towards lesion sites is of vital importance to prevent off-target effects. Various strategies have been employed for targeted therapy, especially in cancer research, where adverse effects are often severe. The different targeting strategies can be categorized in two groups: passive and active targeting. Passive targeting in cancer therapy, is possible because of tumor microenvironments (TMEs), which differ from healthy tissue. Active targeting on the other hand, involves the functionalization of surface moieties of the catalyst/drug nanocarrier with ligands, antibodies or other molecular functionalities, to identify and attach to specific cells, cellular receptors, or tissues.<sup>2</sup> An essential requirement for both passive and active targeting is that nanocarriers are not cleared too rapidly from the bloodstream, thereby providing adequate circulation time. This is typically achieved by applying so-called stealth coatings, which form a hydrated, neutrally charged polymer layer such as PEG or zwitterionic brushes on the particle surface to resist protein adsorption and evade recognition and uptake by the mononuclear phagocyte system.<sup>99</sup> Because of the increasing risk of PEG antigenicity by the immune system, alternative scaffolds to PEG are investigated.<sup>100,101</sup> For example, our group recently reported the decoration of the PEG-termini with charge neutral ylide residue and have shown that recognition by anti-PEG antibodies is diminished.<sup>102,103</sup>

Here, a brief overview is presented how some examples discussed before are equipped with targeting functionalization of the enabling macromolecular scaffold, again highlighting the importance of their use in multimodular strategies.

### 4.1 Passive targeting

As observed, most studies discussed in this review that have been extended to *in vivo* applications, are focused on cancer

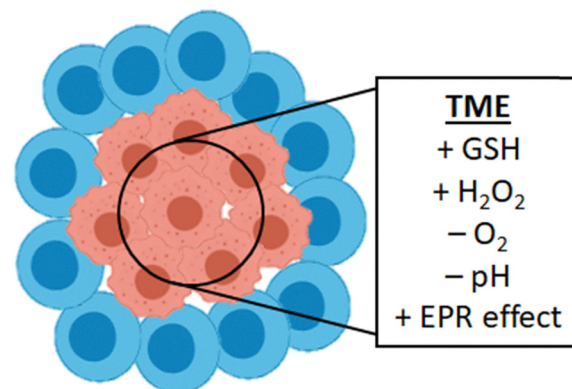


Fig. 14 Tumor tissue is different from healthy tissue and forms a so-called tumor micro-environment (TME). This TME often shows high GSH and hydrogen peroxide concentrations and low oxygen and pH. It also accommodates for the observed EPR effect.

therapy research. In cancer therapy a targeting strategy often applied is passive targeting using properties of the TME that are vastly different from healthy tissue. TMEs are acidic environments and express high glutathione (GSH), high hydrogen peroxide ( $\text{H}_2\text{O}_2$ ), and low oxygen (hypoxia) contents (Fig. 14).<sup>104</sup> The complex TME can form great barriers towards drug delivery to tumors. However, because of its differences with healthy tissue it can also be utilized for targeted drug therapy.<sup>105,106</sup> One property of the TME that is often utilized is the leaky vasculature and impaired lymphatic drainage. This property leads to the enhanced permeability and retention (EPR) effect, first observed by Maeda and Matsumura in the 1980s.<sup>107,108</sup> In some cancers, this effect causes macromolecules (liposomes, nanoparticles, macromolecules) to preferentially accumulate in tumor tissue as compared to healthy tissue, to sustain and stimulate the rapid growth of cancer cells. This effect can subsequently be abused to passively accumulate drug nanocarriers, nanozymes, or in our case, nanoparticle bioorthogonal catalysts at tumor sites, resulting in concentrations high enough for therapeutic efficacy.<sup>109</sup> EPR targeted anti-cancer therapy through *in situ* mediated bond-forming drug synthesis has been shown for polymer based Pd-catalyst NPs,<sup>31</sup> Pd-functionalized CuS nanoplatelets,<sup>96</sup> Cu-NP functionalized mesoporous carbon nanospheres<sup>91</sup> and polymer based copper nanocomplexes.<sup>98</sup> In cases of the latter three examples tumor targeting control using the EPR effect was combined with external stimuli for additional spatiotemporal control using NIR and US irradiation (*vide supra*). Although this targeting strategy seems promising, it must be noted that there are significant physiological differences between rodents and humans and its success can not directly be assumed in human clinical trials.

Some studies utilize specific factors from the TME to selectively activate their catalyst. Studies that use the GSH, and  $\text{H}_2\text{O}_2$  overexpression in TMEs to target catalyst delivery and activation have been presented in this review.

Biocompatible CuAl-LDH nanosheets utilize both EPR and TME for targeting. The nanosheets are first accumulated in tumor tissue *via* the EPR effect and consequently reduced *via* high GSH concentration to form Cu(i) for CuAAC promoted



prodrug activation and the generation of ROS because of the presence of high  $H_2O_2$  content.<sup>26</sup> The application of cross-linked lipoic acid nanocapsules (**c**LANCs) also uses the TME for targeted catalyst release. Upon coming into contact with tumoral GSH, the **c**LANCs structure was disrupted resulting in catalyst and prodrug release and consequent *in situ* drug activation.<sup>47</sup> Bimetallic Cu/Zn MOF based on zeolitic imidazolate framework-8 (ZIF-8) also uses both EPR and TME for its targeted activation. After EPR induced accumulation at the tumor, the release is effectuated by the acidity of the TME, dissolving the ZIF-8 and releasing the Zn and Cu ions to work their magic.<sup>24</sup>

One similar approach, not targeted to TMEs but Alzheimer's Disease (AD) generated microenvironments, utilizes elevated  $H_2O_2$  due to amyloid- $\beta$  (A $\beta$ ) aggregation and copper accumulation. Prodrug carrying mesoporous silica nanoparticles can penetrate the blood-brain barrier and disassemble under the AD elevated  $H_2O_2$ , releasing its contents, followed by the endogenous copper mediated prodrug activation and subsequent A $\beta$ -plaque dissociation.<sup>51</sup>

#### 4.2 Active targeting

Active targeting utilizes ligands, antibodies, or other molecular functionalities to specifically target, identify and attach specific cells, cellular receptors, or tissues. Different tissues and cell types often display different receptor expressions because of their different bodily functions. Diseased tissues such as cancer also differ from normal tissues in their receptor expression, because of their hypermetabolism.<sup>110</sup> By modifying NPs with ligands for molecular recognition of these overexpressed receptors, cellular uptake is increased and thereby the therapy efficiency enhanced. Various types of ligands can be employed for this purpose, such as proteins, polysaccharides, nucleic acids, peptides, and small molecules.<sup>111</sup> Active targeting has been applied in *in vivo* drug synthesis studies of which a small selection of examples is discussed in this review. The rapid development of new click reactions for the decoration of complex molecules has significantly advanced the field<sup>112</sup> and many bioconjugation approaches are frequently used to decorate macromolecular scaffolds with targeting residues (Fig. 15).<sup>113</sup>

**4.2.1 Targeting peptides.** Integrin receptors are often highly overexpressed in cancer cells and therefore form an excellent target for drug delivery. The peptide arginine-glycine-aspartic acid (RGD) is commonly used as a targeting ligand for integrin receptors.<sup>114</sup> This strategy was used in the targeted delivery of the albumin-based Ru-ArM functionalized with cyclic RGD (cRGD) in SW620-xenografted mice and resulted in high tumor growth inhibition due to the targeting strategy. This was evident from better results using targeted *in situ* synthesis than non-targeted drug administration.<sup>61</sup> Pd-nanoparticles functionalized with cRGD, have displayed excellent selectivity for integrin-positive cell line U87-MG over integrin-negative cell line MCF-7 ( $>95\% \text{ vs. } <4\%$  cellular uptake).<sup>55</sup> Another example is the targeted delivery of the metallopeptide HRGDH-Pd which consisted of the RGD

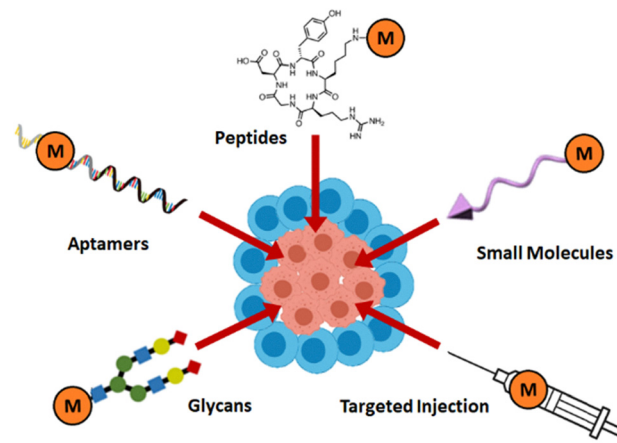


Fig. 15 Various active targeting strategies have been reported in combination with *in situ* bond forming drug synthesis including the use of targeting glycans, aptamers, peptides, small molecules, and targeted injection. M = Macromolecular scaffold with embedded catalyst.

sequence sandwiched between two Pd-chelating histidine (H) moieties. Using this targeted metallopeptide, the stable NHC-Au complex could selectively be transmetallated and activated in integrin-overexpressing HeLa cells, resulting in a 12-fold efficiency improvement over healthy LO2 cells.

**4.2.2 Targeting aptamers.** Nucleic acid aptamers are short sequences of RNA or DNA that bind specific molecules, proteins or receptors.<sup>115</sup> Aptamers have been used in targeted delivery of DNA based nanoparticles discussed before (*vide supra*). For example, the aptamer AS1411 has great affinity for nucleolin, overexpressed in cancer cells, and has therefore been used in tumor targeting strategies. It was used for targeted delivery of **DNzyme**-Cu-NPs to HeLa tumors in mice for *in situ* drug synthesis therapy with great efficiency.<sup>27</sup> The aptamer MUC1, specific for the Mucin1 receptor uniquely and abundantly expressed in adenocarcinoma cells,<sup>116</sup> was also utilized for targeted delivery of DNA-templated Cu-NP. The catalyst was selectively delivered to MUC1-positive tumors in mice for *in situ* drug synthesis, with incredible antitumor effects.<sup>52</sup> The adenosine triphosphate (ATP) aptamer targets high levels of ATP in tumor tissue. This aptamer was used to coat the ZIF-90 MOF employed for targeted prodrug delivery to tumors in 4T1 tumor bearing mice. Upon ATP binding, the MOF would 'melt' due to ATP binding of the Zn(II) bound ZIF-90, releasing the contents for *in situ* synthesis resulting in tumor growth inhibition.<sup>50</sup>

**4.2.3 Targeting glycans.** Glycan functionalized proteins have been shown to be able to efficiently accumulate in different organs (liver, intestine, spleen) depending on glycan structure, due to their affinity for specific glycoproteins and lectins.<sup>117</sup>

Additionally, glycans have been shown to be able to effectuate tumor specific accumulation as well.<sup>118</sup> This strategy has been employed for *in situ* drug synthesis to selectively accumulate glycoalbumin based **Au-GArMs** in liver and intestine for *in vivo* Au-mediated fluorescence labeling and ref. 34, **Ru-GArMs** in SW620 colon adenocarcinoma cells and in HeLa tumors in

mice for metathesis mediated *in situ* and *in vivo* drug synthesis,<sup>18,33</sup> and Au-GArMs in SW620 cells for hydroamination cyclization mediated *in situ* drug synthesis.<sup>35</sup>

**4.2.4 Targeting small molecules.** The folate receptor is often overexpressed on cancer cells because folic acid is essential for the generation of nucleotides and therefore consumed in high quantity by cancer cells.<sup>119</sup> Therefore, the folate receptor is a good target for anti-cancer therapy.<sup>120</sup> Using this strategy, a *cis*-platin Cu chaperone mimic MOF functionalized with folic acid moieties, was efficiently endocytosed in B16F10 melanoma tumors in mice, where they induced copper accumulation and subsequent prodrug activation for successful tumor growth inhibition.<sup>25</sup> The use of a MOF as nanocarrier enabled straightforward targeting functionalization.

**4.2.5 Localized injection.** The most simple and straightforward method of targeted drug delivery is targeted injection, where an implantable device is specifically injected in targeted tissue to exert its function locally. This was done with Cu-NPs entrapped in a TentaGel resin to locally induce *in situ* CuAAC promoted fluorescence in zebrafish yolk sacs after injection of a single bead. Due to the relatively large size of the bead (160.4 ± 10.3 μm) no translocation was possible resulting in localized catalysis.<sup>19</sup> This could be a good strategy for the targeted delivery in hard-to-reach solid tumor deep tissue.

## 5. Conclusions and outlook

*In situ* bioorthogonal synthesis of drug molecules opens new doors in the fields of cell biology and biomedicine. With the introduction of many new-to-nature reactions to *in vivo* systems, possibilities arise for the invention of new techniques for the interrogation and alteration of cells and their metabolism, but also new therapy strategies, enhancing efficiency, specificity, and selectivity ultimately leading to higher efficacy and the reduction of side effects.

Currently, the research in the field of *in situ* synthesis is mainly focused on the development of new bioorthogonal chemistries and application strategies. Hereby, a significant move is being made towards the optimization of physiological stability of the catalytic systems, and target specificity through smart combination with known targeting strategies for *in vivo* application. Currently, studies towards new bioorthogonal bond-forming chemistries are rapidly emerging. These chemistries have been shown to be possible under aqueous and/or biologically relevant media *in vitro* and therefore show potential use for *in situ* synthesis for *in vivo* applications. For example, the authors consider a range of reactions including copper catalyzed Diels–Alder cycloaddition,<sup>121</sup> Friedel–Crafts alkylation,<sup>122</sup> and nitrene transfer sulfimidation,<sup>123</sup> palladium-only catalyzed Sonogashira coupling,<sup>124–126</sup> ruthenium catalyzed atroposelective metathesis,<sup>127</sup> alkyne–alkene coupling,<sup>128,129</sup> and (light-induced) deboronative, and decarboxylative alkynylation,<sup>130,131</sup> and azide–thioalkyne cycloaddition,<sup>132,133</sup> and iridium catalyzed 1,3-dipolar cycloadditions of azides with ynamides, internal alkynes, and internal disulfanyl alkynes.<sup>134–136</sup>

The recent past has shown that improved control obtained from bioorthogonal methods is greatly enhanced through the addition of TMC promoted reactions. Notably, the addition of new functionalities for spatiotemporal control through exogenous stimulation may result in even higher specificity and efficacy. As highlighted, the need for nano-carriers with secondary functionality is essential for both targeting functionalization and exogenous stimulation as well as for shielding of catalyst functionality. The research presented in this review shows immense potential for future clinical applications, especially evident from some highly effective cancer therapy strategies in mice studies. Synergistic multi-modal therapy strategies are in this case most prominent, especially for diseases like cancer with multifactorial origins.

One aspect of *in situ* synthesis that so far has remained under-explored is the concept of ‘retrosynthetic prodrug design’ as introduced by Tanaka.<sup>18</sup> The advantage of *in situ* synthesis, is the possibility to design the ideal prodrug utilizing all possible bioorthogonal chemistries. To design the ideal prodrug, optimization should be pursued in creating the largest difference in bioactivity between drug and prodrug resulting in higher side effect suppression, but also in reactivity, catalytic efficiency, and bioavailability.

As the field of nanomedicine involving macromolecular scaffolds continues to emerge, regulatory agencies are still adapting their frameworks, and several key challenges remain to be addressed. One critical issue is batch-to-batch consistency, which is essential for ensuring safety, regulatory approval, and the feasibility of large-scale manufacturing.<sup>137</sup> In situ-forming scaffolds including injectable drug depots, pose additional challenges, particularly when self-administered by patients, and require rigorous monitoring for obtaining safety profiles. Another growing concern is the immunogenicity associated with nanomedicines.<sup>138,139</sup> For example, anti-PEG antibodies, whether pre-existing or induced by repeated administration of PEGylated drugs or vaccines, can compromise both the safety and efficacy of nanomedicines. These antibodies may affect biodistribution of nanocarriers, trigger unwanted inflammatory responses, destabilize polymer drug formulations, and in some cases result in hypersensitivity reactions.

Artificial intelligence (AI) holds great promise for advancing the design of macromolecular platforms in nanomedicine. By analyzing complex datasets, AI may help to optimize drug combinations, release profiles, and scaffold architectures to enhance therapeutic outcomes.<sup>140,141</sup> This is particularly valuable for combination therapies, where drug synergy is time-, dose-, and patient-dependent. Unlike fixed-dose approaches, AI may help to guide the development of adaptive nanocarriers tailored to individual needs, enabling more effective and personalized treatments. In context of drug synthesis using metal catalysts, such computational power would be of high value to determine most effective concentrations of drug fragments, taking into account stability and circulation time.

In summary, the introduction of transition metal promoted synthesis in biological systems with the help of macromolecular platforms is primed for remarkable advancements in the coming years.



## Author contributions

TvE revised literature. TvE and KN wrote the manuscript.

## Conflicts of interest

There are no conflicts to declare.

## Data availability

No primary research results, software or code have been included, and no new data were generated or analysed as part of this review.

## Acknowledgements

We like to acknowledge Radboud University for providing access to literature.

## References

- 1 W. M. van den Boogaard, D. S. Komninos and W. P. Vermeij, Chemotherapy side-effects: not all DNA damage is equal, *Cancers*, 2022, **14**(3), 627.
- 2 J. Li, *et al.*, Recent advances in targeted drug delivery strategy for enhancing oncotherapy, *Pharmaceutics*, 2023, **15**(9), 2233.
- 3 K. M. Huttunen, H. Raunio and J. Rautio, Prodrugs—from serendipity to rational design, *Pharmacol. Rev.*, 2011, **63**(3), 750–771.
- 4 Q. Fu, *et al.*, Bioorthogonal chemistry for prodrug activation *in vivo*, *Chem. Soc. Rev.*, 2023, **52**, 7737–7772.
- 5 H. C. Hang, *et al.*, A metabolic labeling approach toward proteomic analysis of mucin-type O-linked glycosylation, *Proc. Natl. Acad. Sci. U. S. A.*, 2003, **100**(25), 14846–14851.
- 6 D. M. Patterson, L. A. Nazarova and J. A. Prescher, Finding the right (bioorthogonal) chemistry, *ACS Chem. Biol.*, 2014, **9**(3), 592–605.
- 7 J. Tu, M. Xu and R. M. Franzini, Dissociative bioorthogonal reactions, *ChemBioChem*, 2019, **20**(13), 1615–1627.
- 8 C. Zhong and X. Shi, When organocatalysis meets transition-metal catalysis, *Eur. J. Org. Chem.*, 2010, (16), 2999–3025.
- 9 H. Madec, *et al.*, Metal complexes for catalytic and photo-catalytic reactions in living cells and organisms, *Chem. Sci.*, 2023, **14**(3), 409–442.
- 10 D. P. Nguyen, H. T. Nguyen and L. H. Do, Tools and methods for investigating synthetic metal-catalyzed reactions in living cells, *ACS Catal.*, 2021, **11**(9), 5148–5165.
- 11 N. K. Devaraj, *et al.*, Reactive polymer enables efficient *in vivo* bioorthogonal chemistry, *Proc. Natl. Acad. Sci. U. S. A.*, 2012, **109**(13), 4762–4767.
- 12 J. M. Mejia Oneto, *et al.*, *In vivo* bioorthogonal chemistry enables local hydrogel and systemic pro-drug to treat soft tissue sarcoma, *ACS Cent. Sci.*, 2016, **2**(7), 476–482.
- 13 D. Karagrigoriou, *et al.*, Unveiling the Antifouling Potential of Stabilized Poly(phosphorus ylides), *ACS Macro Lett.*, 2023, **12**(12), 1608–1613.
- 14 K. Neumann, The case for poly(ylides) as a class of charge-neutral, hydrophilic polymers with applications in biomaterials science, *Biomater. Sci.*, 2024, **12**(21), 5481–5490.
- 15 B. Li, *et al.*, Trimethylamine N-oxide-derived zwitterionic polymers: A new class of ultralow fouling bioinspired materials, *Sci. Adv.*, 2019, **5**(6), eaaw9562.
- 16 K. Neumann, S. Jain, J. Geng and M. Bradley, Nanoparticle “switch-on” by tetrazine triggering, *Chem. Commun.*, 2016, **52**, 11223.
- 17 M. O. van de L'Isle, M. C. Ortega-Liebana and A. Unciti-Broceta, Transition metal catalysts for the bioorthogonal synthesis of bioactive agents, *Curr. Opin. Chem. Biol.*, 2021, **61**, 32–42.
- 18 I. Nasibullin, *et al.*, Synthetic prodrug design enables biocatalytic activation in mice to elicit tumor growth suppression, *Nat. Commun.*, 2022, **13**(1), 39.
- 19 J. Clavadetscher, *et al.*, Copper catalysis in living systems and *in situ* drug synthesis, *Angew. Chem., Int. Ed.*, 2016, **128**(50), 15891–15895.
- 20 J. Huang, *et al.*, Nanocopper-doped cross-linked lipoic acid nanoparticles for morphology-dependent intracellular catalysis, *ACS Catal.*, 2018, **8**(7), 5941–5946.
- 21 Y. Bai, *et al.*, A highly efficient single-chain metal–organic nanoparticle catalyst for alkyne–azide “click” reactions in water and in cells, *J. Am. Chem. Soc.*, 2016, **138**(35), 11077–11080.
- 22 Q. Lu, *et al.*, A dense-shell macromolecular scaffold for catalyst- or substrate-guided catalysis in a cellular environment, *ACS Mater. Lett.*, 2019, **2**(1), 89–94.
- 23 F. Wang, *et al.*, A biocompatible heterogeneous MOF–Cu catalyst for *in vivo* drug synthesis in targeted subcellular organelles, *Angew. Chem., Int. Ed.*, 2019, **58**(21), 6987–6992.
- 24 Z. Wang, *et al.*, A bimetallic metal–organic framework encapsulated with DNAzyme for intracellular drug synthesis and self-sufficient gene therapy, *Angew. Chem.*, 2021, **133**(22), 12539–12545.
- 25 Y. Wei, *et al.*, MOFs Modulate Copper Trafficking in Tumor Cells for Bioorthogonal Therapy, *Nano Lett.*, 2024, **24**(4), 1341–1350.
- 26 S. Wang, *et al.*, *In situ* activation of CuAl-LDH nanosheets to catalyze bioorthogonal chemistry *in vivo* in tumor microenvironment for precise chemotherapy and chemo-dynamic therapy, *Chem. Eng. J.*, 2023, **457**, 141186.
- 27 Y. You, *et al.*, A DNAzyme-augmented bioorthogonal catalysis system for synergistic cancer therapy, *Chem. Sci.*, 2022, **13**(26), 7829–7836.
- 28 R. M. Yusop, *et al.*, Palladium-mediated intracellular chemistry, *Nat. Chem.*, 2011, **3**(3), 239–243.
- 29 E. Indrigo, *et al.*, Palladium-mediated *in situ* synthesis of an anticancer agent, *Chem. Commun.*, 2016, **52**(99), 14212–14214.
- 30 P. Destito, *et al.*, Hollow nanoreactors for Pd-catalyzed Suzuki–Miyaura coupling and O-propargyl cleavage



reactions in bio-relevant aqueous media, *Chem. Sci.*, 2019, **10**(9), 2598–2603.

31 M. A. Miller, *et al.*, Nano-palladium is a cellular catalyst for *in vivo* chemistry, *Nat. Commun.*, 2017, **8**(1), 15906.

32 M. Jeschek, *et al.*, Directed evolution of artificial metalloenzymes for *in vivo* metathesis, *Nature*, 2016, **537**(7622), 661–665.

33 S. Eda, *et al.*, Biocompatibility and therapeutic potential of glycosylated albumin artificial metalloenzymes, *Nat. Catal.*, 2019, **2**(9), 780–792.

34 K. Tsubokura, *et al.*, *In vivo* gold complex catalysis within live mice, *Angew. Chem., Int. Ed.*, 2017, **56**(13), 3579–3584.

35 M. Kurimoto, *et al.*, Anticancer approach inspired by the hepatotoxic mechanism of pyrrolizidine alkaloids with glycosylated artificial metalloenzymes, *Angew. Chem., Int. Ed.*, 2022, **61**(43), e202205541.

36 C. Sambiagio, *et al.*, Copper catalysed Ullmann type chemistry: from mechanistic aspects to modern development, *Chem. Soc. Rev.*, 2014, **43**(10), 3525–3550.

37 A. M. Thomas, A. Sujatha and G. Anilkumar, Recent advances and perspectives in copper-catalyzed Sonogashira coupling reactions, *RSC Adv.*, 2014, **4**(42), 21688–21698.

38 M. M. Heravi, *et al.*, Buchwald-Hartwig reaction: an overview, *J. Organomet. Chem.*, 2018, **861**, 17–104.

39 M. Breugst and H. U. Reissig, The Huisgen reaction: Milestones of the 1,3-dipolar cycloaddition, *Angew. Chem., Int. Ed.*, 2020, **59**(30), 12293–12307.

40 H. C. Kolb, M. Finn and K. B. Sharpless, Click chemistry: diverse chemical function from a few good reactions, *Angew. Chem., Int. Ed.*, 2001, **40**(11), 2004–2021.

41 S. Shaligram and A. Campbell, Toxicity of copper salts is dependent on solubility profile and cell type tested, *Toxicol. In Vitro*, 2013, **27**(2), 844–851.

42 L. M. Gaetke and C. K. Chow, Copper toxicity, oxidative stress, and antioxidant nutrients, *Toxicology*, 2003, **189**(1–2), 147–163.

43 L. Li and Z. Zhang, Development and applications of the copper-catalyzed azide-alkyne cycloaddition (CuAAC) as a bioorthogonal reaction, *Molecules*, 2016, **21**(10), 1393.

44 J. Chen, *et al.*, Enzyme-like click catalysis by a copper-containing single-chain nanoparticle, *J. Am. Chem. Soc.*, 2018, **140**(42), 13695–13702.

45 J. Chen, *et al.*, Polymeric “clickase” accelerates the copper click reaction of small molecules, proteins, and cells, *J. Am. Chem. Soc.*, 2019, **141**(24), 9693–9700.

46 J. Chen, *et al.*, A bioorthogonal small molecule selective polymeric “clickase”, *J. Am. Chem. Soc.*, 2020, **142**(32), 13966–13973.

47 L. Wang, *et al.*, “One-stitch” bioorthogonal prodrug activation based on cross-linked lipoic acid nanocapsules, *Biomaterials*, 2021, **273**, 120823.

48 Y. Deng, *et al.*, A membrane-embedded macromolecular catalyst with substrate selectivity in live cells, *J. Am. Chem. Soc.*, 2022, **145**(2), 1262–1272.

49 H. Furukawa, *et al.*, The chemistry and applications of metal-organic frameworks, *Science*, 2013, **341**(6149), 1230444.

50 J. Zhu, *et al.*, Boosting Endogenous Copper(I) for Biologically Safe and Efficient Bioorthogonal Catalysis *via* Self-Adaptive Metal-Organic Frameworks, *J. Am. Chem. Soc.*, 2023, **145**(3), 1955–1963.

51 Z. Du, *et al.*, Self-triggered click reaction in an Alzheimer’s disease model: *in situ* bifunctional drug synthesis catalyzed by neurotoxic copper accumulated in amyloid- $\beta$  plaques, *Chem. Sci.*, 2019, **10**(44), 10343–10350.

52 Y. You, *et al.*, DNA-based platform for efficient and precisely targeted bioorthogonal catalysis in living systems, *Nat. Commun.*, 2022, **13**(1), 1459.

53 A. Biffis, *et al.*, Pd metal catalysts for cross-couplings and related reactions in the 21st century: a critical review, *Chem. Rev.*, 2018, **118**(4), 2249–2295.

54 J. G. Rebelein and T. R. Ward, *In vivo* catalyzed new-to-nature reactions, *Curr. Opin. Biotechnol.*, 2018, **53**, 106–114.

55 J. Clavadetscher, *et al.*, In-Cell Dual Drug Synthesis by Cancer-Targeting Palladium Catalysts, *Angew. Chem.*, 2017, **129**(24), 6968–6972.

56 A. M. Pérez-López, *et al.*, Dual-bioorthogonal catalysis by a palladium peptide complex, *J. Med. Chem.*, 2023, **66**(5), 3301–3311.

57 J. Hafeez, *et al.*, Synthesis of ruthenium complexes and their catalytic applications: A review, *Arabian J. Chem.*, 2022, **15**(11), 104165.

58 G. C. Vougioukalakis and R. H. Grubbs, Ruthenium-based heterocyclic carbene-coordinated olefin metathesis catalysts, *Chem. Rev.*, 2010, **110**(3), 1746–1787.

59 T. R. Ward, Artificial metalloenzymes based on the biotin–avidin technology: enantioselective catalysis and beyond, *Acc. Chem. Res.*, 2011, **44**(1), 47–57.

60 H. Kruszyna, *et al.*, Toxicology and pharmacology of some ruthenium compounds: Vascular smooth muscle relaxation by nitrosyl derivatives of ruthenium and iridium, *J. Toxicol. Environ. Health, Part A*, 1980, **6**(4), 757–773.

61 I. Nasibullin, *et al.*, Catalytic olefin metathesis in blood, *Chem. Sci.*, 2023, **14**(40), 11033–11039.

62 A. S. K. Hashmi, Gold-catalyzed organic reactions, *Chem. Rev.*, 2007, **107**(7), 3180–3211.

63 S. R. Thomas and A. Casini, Gold compounds for catalysis and metal-mediated transformations in biological systems, *Curr. Opin. Chem. Biol.*, 2020, **55**, 103–110.

64 T. C. Chang, *et al.*, Prodrug Activation by Gold Artificial Metalloenzyme-Catalyzed Synthesis of Phenanthridinium Derivatives *via* Hydroamination, *Angew. Chem., Int. Ed.*, 2021, **133**(22), 12554–12562.

65 S. B. Singh, Iridium chemistry and its catalytic applications: A brief, *Green Chem. Technol.*, 2016, **2**(206), 456–518.

66 Y. Okamoto and T. R. Ward, Transfer hydrogenation catalyzed by organometallic complexes using NADH as a reductant in a biochemical context, *Biochemistry*, 2017, **56**(40), 5223–5224.

67 N. Singh, *et al.*, Iridium-triggered allylcarbamate uncaging in living cells, *Inorg. Chem.*, 2021, **60**(17), 12644–12650.

68 C. Huang, *et al.*, *In vitro* and *in vivo* photocatalytic cancer therapy with biocompatible iridium(III) photocatalysts, *Angew. Chem.*, 2021, **133**(17), 9560–9565.



69 Z. Liu, *et al.*, Assembly and Evolution of Artificial Metalloenzymes within *E. coli Nissle* 1917 for Enantioselective and Site-Selective Functionalization of C–H and C=C Bonds, *J. Am. Chem. Soc.*, 2022, **144**(2), 883–890.

70 J. Huang, *et al.*, Unnatural biosynthesis by an engineered microorganism with heterologously expressed natural enzymes and an artificial metalloenzyme, *Nat. Chem.*, 2021, **13**(12), 1186–1191.

71 H. M. Key, *et al.*, Abiological catalysis by artificial haem proteins containing noble metals in place of iron, *Nature*, 2016, **534**(7608), 534–537.

72 S. Wallace and E. P. Balskus, Interfacing microbial styrene production with a biocompatible cyclopropanation reaction, *Angew. Chem., Int. Ed.*, 2015, **54**(24), 7106–7109.

73 P. S. Coelho, *et al.*, A serine-substituted P450 catalyzes highly efficient carbene transfer to olefins *in vivo*, *Nat. Chem. Biol.*, 2013, **9**(8), 485–487.

74 S. J. Kan, *et al.*, Directed evolution of cytochrome *c* for carbon–silicon bond formation: Bringing silicon to life, *Science*, 2016, **354**(6315), 1048–1051.

75 K. Chen, *et al.*, Enzymatic construction of highly strained carbocycles, *Science*, 2018, **360**(6384), 71–75.

76 M. Garcia-Borràs, *et al.*, Origin and control of chemoselectivity in cytochrome *c* catalyzed carbene transfer into Si–H and N–H bonds, *J. Am. Chem. Soc.*, 2021, **143**(18), 7114–7123.

77 Z. Liu, *et al.*, Dual-function enzyme catalysis for enantioselective carbon–nitrogen bond formation, *Nat. Chem.*, 2021, **13**(12), 1166–1172.

78 A. L. Chandgude, X. Ren and R. Fasan, Stereodivergent intramolecular cyclopropanation enabled by engineered carbene transferases, *J. Am. Chem. Soc.*, 2019, **141**(23), 9145–9150.

79 X. Ren, A. L. Chandgude and R. Fasan, Highly stereoselective synthesis of fused cyclopropane- $\gamma$ -lactams via biocatalytic iron-catalyzed intramolecular cyclopropanation, *ACS Catal.*, 2020, **10**(3), 2308–2313.

80 K. Fagnou and M. Lautens, Rhodium-catalyzed carbon–carbon bond forming reactions of organometallic compounds, *Chem. Rev.*, 2003, **103**(1), 169–196.

81 H. T. Chifotides and K. R. Dunbar, Interactions of metal–metal-bonded antitumor active complexes with DNA fragments and DNA, *Acc. Chem. Res.*, 2005, **38**(2), 146–156.

82 J. Zhao, *et al.*, An artificial metalloenzyme for carbene transfer based on a biotinylated dirhodium anchored within streptavidin, *Catal. Sci. Technol.*, 2018, **8**(9), 2294–2298.

83 K. A. Mix, M. R. Aronoff and R. T. Raines, Diazo compounds: versatile tools for chemical biology, *ACS Chem. Biol.*, 2016, **11**(12), 3233–3244.

84 Z. T. Ball, Molecular recognition in protein modification with rhodium metallopeptides, *Curr. Opin. Chem. Biol.*, 2015, **25**, 98–102.

85 Z. Zhao, *et al.*, Dual stimulus-triggered bioorthogonal nanosystem for spatiotemporally controlled prodrug activation and near-infrared fluorescence imaging, *Chem. Commun.*, 2023, **59**(26), 3878–3881.

86 Y. Zhang, *et al.*, Nanoparticulation of prodrug into medicines for cancer therapy, *Adv. Sci.*, 2021, **8**(18), 2101454.

87 K. Neumann, A. Lilienkampf and M. Bradley, Responsive polymeric nanoparticles for controlled drug delivery, *Polym. Int.*, 2017, **66**(12), 1756–1764.

88 N. Mamidi, *et al.*, Carbonaceous nanomaterials incorporated biomaterials: The present and future of the flourishing field, *Composites, Part B*, 2022, **243**, 110150.

89 C. I. Crucho, Stimuli-responsive polymeric nanoparticles for nanomedicine, *ChemMedChem*, 2015, **10**(1), 24–38.

90 N. Mamidi, F. F. De Silva and A. O. M. Salehi, Advanced disease therapeutics using engineered living drug delivery systems, *Nanoscale*, 2025, **17**, 7673–7696.

91 Y. You, *et al.*, Near-infrared light dual-promoted heterogeneous copper nanocatalyst for highly efficient bioorthogonal chemistry *in vivo*, *ACS Nano*, 2020, **14**(4), 4178–4187.

92 P. A. Shaw, *et al.*, Two-photon absorption: an open door to the NIR-II biological window?, *Front. Chem.*, 2022, **10**, 921354.

93 R. Weissleder, A clearer vision for *in vivo* imaging, *Nat. Biotechnol.*, 2001, **19**(4), 316–317.

94 R. C. Remmers and K. Neumann, Reaching new lights: a review on photo-controlled nanomedicines and their *in vivo* evaluation, *Biomater. Sci.*, 2023, **11**(5), 1607–1624.

95 F. Wang, *et al.*, Designed heterogeneous palladium catalysts for reversible light-controlled bioorthogonal catalysis in living cells, *Nat. Commun.*, 2018, **9**(1), 1209.

96 H. Zhao, *et al.*, NIR-II light leveraged dual drug synthesis for orthotopic combination therapy, *ACS Nano*, 2022, **16**(12), 20353–20363.

97 J. Lee, *et al.*, Magnetothermia-induced catalytic hollow nanoreactor for bioorthogonal organic synthesis in living cells, *Nano Lett.*, 2020, **20**(10), 6981–6988.

98 L. Xia, *et al.*, Spatiotemporal ultrasound-driven bioorthogonal catalytic therapy, *Adv. Mater.*, 2023, **35**(7), 2209179.

99 G. Pasut and F. M. Veronese, PEG conjugates in clinical development or use as anticancer agents: an overview, *Adv. Drug Delivery Rev.*, 2009, **61**(13), 1177–1188.

100 A. S. A. Lila, H. Kiwada and T. Ishida, The accelerated blood clearance (ABC) phenomenon: clinical challenge and approaches to manage, *J. Controlled Release*, 2013, **172**(1), 38–47.

101 J. J. Verhoef, *et al.*, Potential induction of anti-PEG antibodies and complement activation toward PEGylated therapeutics, *Drug Discovery Today*, 2014, **19**(12), 1945–1952.

102 G. Poullandofonou and K. Neumann, Poly(sulfur ylides): a new class of zwitterionic polymers with distinct thermal and solution behaviour, *Polym. Chem.*, 2022, **13**(30), 4416–4420.

103 D. M. Sánchez-Cerrillo, *et al.*, Introducing Ylides as Charge-Neutral Termini for Poly(Ethylene Glycol) with Applications in Nanomedicine. 2025.

104 E. Henke, R. Nandigama and S. Ergün, Extracellular matrix in the tumor microenvironment and its impact on cancer therapy, *Front. Mol. Biosci.*, 2020, **6**, 160.

105 R. Zhang, *et al.*, Tumor microenvironment-responsive BSA nanocarriers for combined chemo/chemodynamic cancer therapy, *J. Nanobiotechnol.*, 2022, **20**(1), 223.



106 Y. Zhou, *et al.*, Overcoming the biological barriers in the tumor microenvironment for improving drug delivery and efficacy, *J. Mater. Chem. B*, 2020, **8**(31), 6765–6781.

107 Y. Matsumura and H. Maeda, A new concept for macromolecular therapeutics in cancer chemotherapy: mechanism of tumoritropic accumulation of proteins and the antitumor agent smancs, *Cancer Res.*, 1986, **46**(12\_Part\_1), 6387–6392.

108 H. Maeda and Y. Matsumura, Tumoritropic and lymphotropic principles of macromolecular drugs, *Crit. Rev. Ther. Drug Carrier Syst.*, 1989, **6**(3), 193–210.

109 R. Bazak, *et al.*, Passive targeting of nanoparticles to cancer: A comprehensive review of the literature, *Mol. Clin. Oncol.*, 2014, **2**(6), 904–908.

110 F. S. Anarjan, Active targeting drug delivery nanocarriers: Ligands, *Nano-Struct. Nano-Objects*, 2019, **19**, 100370.

111 J. Yoo, *et al.*, Active targeting strategies using biological ligands for nanoparticle drug delivery systems, *Cancers*, 2019, **11**(5), 640.

112 K. Gavriel, *et al.*, Click'n lock: rapid exchange between unsymmetric tetrazines and thiols for reversible, chemoselective functionalisation of biomolecules with on-demand bioorthogonal locking, *RSC Chem. Biol.*, 2023, **4**(9), 685–691.

113 W. Yi, *et al.*, Recent advances in developing active targeting and multi-functional drug delivery systems *via* bioorthogonal chemistry, *Signal Transduction Targeted Ther.*, 2022, **7**(1), 386.

114 Y. Cheng and Y. Ji, RGD-modified polymer and liposome nanovehicles: Recent research progress for drug delivery in cancer therapeutics, *Eur. J. Pharm. Sci.*, 2019, **128**, 8–17.

115 X. Ni, *et al.*, Nucleic acid aptamers: clinical applications and promising new horizons, *Curr. Med. Chem.*, 2011, **18**(27), 4206–4214.

116 M. Brayman, A. Thathiah and D. D. Carson, MUC1: a multifunctional cell surface component of reproductive tissue epithelia, *Reprod. Biol. Endocrinol.*, 2004, **2**, 1–9.

117 A. Ogura, *et al.*, Visualizing trimming dependence of biodistribution and kinetics with homo- and heterogeneous N-glycoclusters on fluorescent albumin, *Sci. Rep.*, 2016, **6**(1), 21797.

118 A. Ogura, *et al.*, Glycan multivalency effects toward albumin enable N-glycan-dependent tumor targeting, *Bioorg. Med. Chem. Lett.*, 2016, **26**(9), 2251–2254.

119 K. Urbiola, *et al.*, Efficient serum-resistant lipopolyplexes targeted to the folate receptor, *Eur. J. Pharm. Biopharm.*, 2013, **83**(3), 358–363.

120 B. A. Gruner and S. D. Weitman, The folate receptor as a potential therapeutic anticancer target, *Invest. New Drugs*, 1998, **16**, 205–219.

121 W. Ghattas, *et al.*, Receptor-based artificial metalloenzymes on living human cells, *J. Am. Chem. Soc.*, 2018, **140**(28), 8756–8762.

122 S. Chordia, *et al.*, *In vivo* assembly of artificial metalloenzymes and application in whole-cell biocatalysis, *Angew. Chem., Int. Ed.*, 2021, **60**(11), 5913–5920.

123 E. J. Meeus, *et al.*, Copper-Catalyzed Sulfimidation in Aqueous Media: a Fast, Chemoselective and Biomolecule-Compatible Reaction, *Chem. – Eur. J.*, 2024, **30**(14), e202303939.

124 N. Li, *et al.*, Copper-free Sonogashira cross-coupling for functionalization of alkyne-encoded proteins in aqueous medium and in bacterial cells, *J. Am. Chem. Soc.*, 2011, **133**(39), 15316–15319.

125 J. Li, *et al.*, Ligand-free palladium-mediated site-specific protein labeling inside Gram-negative bacterial pathogens, *J. Am. Chem. Soc.*, 2013, **135**(19), 7330–7338.

126 N. Li, *et al.*, A genetically encoded alkyne directs palladium-mediated protein labeling on live mammalian cell surface, *ACS Chem. Biol.*, 2015, **10**(2), 379–384.

127 T. Vornholt, *et al.*, An Artificial Metalloenzyme for Atroposelective Metathesis, *ChemCatChem*, 2023, **15**(23), e202301113.

128 L. Adriaenssens, *et al.*, Bio- and air-tolerant carbon–carbon bond formations *via* organometallic ruthenium catalysis, *Collect. Czech. Chem. Commun.*, 2009, **74**(7), 1023–1034.

129 A. Gutiérrez-González, *et al.*, Ruthenium-catalyzed intermolecular alkene–alkyne couplings in biologically relevant media, *Chem. Sci.*, 2023, **14**(23), 6408–6413.

130 H. Huang, *et al.*, Visible-light-induced chemoselective deboronative alkynylation under biomolecule-compatible conditions, *J. Am. Chem. Soc.*, 2014, **136**(6), 2280–2283.

131 J. Yang, *et al.*, Visible-light-induced chemoselective reductive decarboxylative alkynylation under biomolecule-compatible conditions, *Chem. Commun.*, 2015, **51**(25), 5275–5278.

132 P. Destito, *et al.*, Ruthenium-Catalyzed Azide–Thioalkyne Cycloadditions in Aqueous Media: A Mild, Orthogonal, and Biocompatible Chemical Ligation, *Angew. Chem., Int. Ed.*, 2017, **56**(36), 10766–10770.

133 A. Gutiérrez-González, *et al.*, Bioorthogonal Azide–Thioalkyne Cycloaddition Catalyzed by Photoactivatable Ruthenium(II) Complexes, *Angew. Chem., Int. Ed.*, 2021, **60**(29), 16059–16066.

134 W. Song and N. Zheng, Iridium-catalyzed highly regioselective azide–ynamide cycloaddition to access 5-amido Fully substituted 1, 2, 3-triazoles under mild, air, aqueous, and bioorthogonal conditions, *Org. Lett.*, 2017, **19**(22), 6200–6203.

135 R. Chen, *et al.*, Iridium-Catalyzed Hydroxyl-Enabled Cycloaddition of Azides and Alkynes, *Adv. Synth. Catal.*, 2019, **361**(5), 989–994.

136 M. Li, *et al.*, Iridium-catalyzed orthogonal and regioselective synthesis of triazole disulfides in aqueous media under mild conditions, *Green Chem.*, 2020, **22**(8), 2394–2398.

137 N. Mamidi, *et al.*, Innovative hydrogel-based delivery systems for immunotherapy: A review of pre-clinical progress, *Nano Res.*, 2024, **17**(10), 9031–9043.

138 Y. Chen, Y.-C. Su and S. R. Roffler, Polyethylene glycol immunogenicity in nanomedicine, *Nat. Rev. Bioeng.*, 2025, 1–19.



139 B.-M. Chen, T.-L. Cheng and S. R. Roffler, Polyethylene glycol immunogenicity: theoretical, clinical, and practical aspects of anti-polyethylene glycol antibodies, *ACS Nano*, 2021, **15**(9), 14022–14048.

140 D. Ho, P. Wang and T. Kee, Artificial intelligence in nanomedicine, *Nanoscale Horiz.*, 2019, **4**(2), 365–377.

141 N. Serov and V. Vinogradov, Artificial intelligence to bring nanomedicine to life, *Adv. Drug Delivery Rev.*, 2022, **184**, 114194.

